When Does the IC_{50} Accurately Assess the Blocking Potency of a Drug?

Julio Gomis-Tena[a], Brandon M. Brown[b], Jordi Cano[a], Beatriz Trenor[a], Pei-Chi Yang[b], Javier Saiz[a], Colleen E. Clancy[b], Lucia Romero[a].*

[a]Centro de Investigación e Innovación en Bioingeniería (Ci2B), Universitat Politècnica de València, Camino de Vera, s/n, 46022, Valencia, Spain.

[b]Department of Pharmacology, One Shields Avenue, University of California, Davis, Davis, CA 95616-8636

ABSTRACT: Preclinical assessment of drug-induced proarrhythmicity is typically evaluated by the potency of the drug to block the potassium human ether-à-go-go-related gene (hERG) channels, which is currently quantified by the IC_{50}. However, channel block depends on the experimental conditions. Our aim is to improve the evaluation of the blocking potency of drugs by designing experimental stimulation protocols to measure the IC_{50} that will help to decide whether the IC_{50} is representative enough. We used the state-of-the-art mathematical models of the cardiac electrophysiological activity to design three stimulation protocols that enhance the differences in the probabilities to occupy a certain conformational state of the channel and, therefore, the potential differences in the blocking effects of a compound. We simulated an extensive set of 144 *in silico* I_{Kr} blockers with different kinetics and affinities to conformational states of the channel

and we also experimentally validated our key predictions. Our results show that the IC_{50} protocol dependency relied on the tested compounds. Some of them showed no differences or small differences on the IC_{50} value, which suggests that the IC_{50} could be a good indicator of the blocking potency in these cases. However, others provided highly protocol dependent IC_{50} values, which could differ even two orders of magnitude. Moreover, the protocols yielding the maximum IC_{50} and minimum IC_{50} depended on the drug, which complicates the definition of a "standard" protocol to minimize the influence of the stimulation protocol on the IC_{50} measurement in safety pharmacology. As a conclusion, we propose the adoption of our three-protocol IC_{50} assay to estimate the potency to block hERG *in vitro*. If the IC_{50} values obtained for a compound are similar, then the IC_{50} could be used as an indicator of its blocking potency, otherwise kinetics and state-dependent binding properties should be accounted.

TEXT

1. Introduction

The rapid component of delayed rectifier current (I_{Kr}), which is encoded by the human ether-à-go-go-related gene (hERG), plays an important role on the cardiac action potential (AP) duration (APD). This current is a well-known promiscuous drug target, and many drugs associated with torsade de pointes (TdP) inhibit the I_{Kr} and hERG channels[1]. Therefore, a key test of the current cardiac safety assessment of pharmacological compounds consists of the observed *in vitro* block of these channels[2]. This is typically quantified by the IC_{50}, which is the drug concentration that blocks 50% of the current. There is experimental evidence of the IC_{50} dependency on the experimental conditions, such as voltage stimulus protocol, temperature and expression system[3–7]. Indeed, hERG channel blockers can inhibit the channel by means of different mechanisms, which may exhibit time, voltage and state dependence[5,8,9]. However, there is no standardization of these

assays at present, which favors the existence of a high variability of the IC_{50} values reported in the literature and databases, such as FDA drug labels, PubChem[10], and DrugBank[11]. A few experimental works have compared the IC_{50} values using different voltage protocols and have reported variations in the IC_{50} values up to 10-fold when only changing the voltage protocol[4–6,12]. However, the number of drugs used in these studies was reduced. A very recent investigation of the factors that contribute to the IC_{50} differences has been performed using a *in silico* drugs binding and unbinding to the open and inactivated states not allowing drug bound channels to change their conformational state[13]. With these simple drug channel interactions, the authors have elegantly shown that state dependence of drug binding is a major determinant of the protocol dependence of I_{Kr} IC_{50}. However, that study only considered *in silico* drugs binding and unbinding in the open and/or inactivated states, not in the closed state, despite of the existence of compounds, such as ketoconazole and BeKm-1, that preferentially block the channel in the closed state[5,8,9]. In addition, drug bound channels in that study were not allowed to change their conformational state, which avoids simulation of drug trapping, a very well-known phenomenon that takes place in the presence of certain drugs[14,15].

Here, we attempt to shed light on the relevance of the IC_{50} as an indicator of the I_{Kr} blocking potency of a compound and to improve the characterization of its blocking effects using a highly detailed Markov model considering a wide range of drug channel interactions. We hypothesize that, as drug-channel interaction may depend on the conformational state of the channel, stimulation at certain voltages where the probability of these states is very different will provide more information about the blocking potency than a unique voltage clamp protocol. In this work, we designed voltage protocols that could unmask distinct state-dependent potencies of block. Then, we systematically carried out "*in silico* drug genesis" by creating a wide range of virtual

drugs with different kinetics and affinities to the conformational states of the I_{Kr} channel. *In silico* drugs are able to bind and unbind to any conformational state of the channel: closed, open and/or inactivated. Moreover, two kinds of drug bound channels were simulated: those that do not change their conformational state and those that do it, which allows simulation of drug trapping. Next, we obtained the Hill-plots for each virtual drug using our new protocols as well as other existing protocols and calculated the IC_{50}s. Finally, we performed some experiments to support our simulation results.

2. Materials and Methods

2.1 Drug models

The human ventricular I_{Kr} was simulated using the five-state Markov chain proposed by Fink et al.[16]. This model has five states: three closed states (C3, C2 and C1), an open state (O) and an inactivated state (I). In order to simulate drug interactions with I_{Kr}, we included the new states the channel can occupy in the presence of the drug, namely, C_{3d}, C_{2d}, C_{1d}, O_d and I_d. Figure 1 shows the simulated I_{Kr} Markov model for multiple drug bound configurations together with the corresponding type drug-channel interaction label. As ion channel targeting drugs display complex properties determined by preferential binding to distinct conformational states and/or distinct affinity to discrete states, we simulated a wide variety of likely drug–channel interactions: drugs that exclusively interact in the closed (Figures 1A and 1B), open (Figures 1C and 1D) or inactivated (Figures 1E and 1F) states, drugs binding simultaneously to both the closed and open states (Figures 1G and 1H), or to both the open and inactivated states (Figures 1I and 1J) and drugs binding simultaneously to all states (Figures 1K and 1L). We allowed drug bound channels to change their conformational state (Figures 1A, 1C, 1E, 1G, 1I and 1K) as in our previous work[17], and we labelled them unstuck, but we also considered the possibility that the drug bound channels

do not change their conformational state unless unbinding occurs, and we labelled them stuck (Figures 1B, 1D, 1F, 1H, 1J and 1L). Microscopic reversibility was ensured by equaling the product of the rates going clockwise to the product going anticlockwise in closed loops[18]. As drug-bound channels are electrically silent, which precludes the assessment of the transition rates between states, we modified the transition rates from I_d to O_d and from O_d to $C1_d$ when appropriate. Drug kinetics were also analyzed in detail by testing a range of diffusion (k) and dissociation rates (r) for the various drug configurations. Dissociation rates ranged from 0.001 to 1000 s^{-1} using logarithmic or half-logarithmic increments, in line with other simulation works[19,20], and the diffusion was the same in all the states where the drug binds. A total of 144 prototypical drugs were simulated, and their names were generated depending on the states the drug binds and unbinds to and the speed of the dissociation rates. We called Closed, Open, and Inactivated drugs to those binding exclusively to the closed, open, or inactivated states, respectively. We labelled ClosedO, OpenC and CO the drugs binding simultaneously to both the open and closed states with higher affinity to the closed state, to the open state, and with the same affinity, respectively. We labelled OpenI, InactivO and IO the drugs binding simultaneously to both the open and inactivated states with higher affinity to the open state, to the inactivated state, and with the same affinity, respectively. Finally, we labelled COI, ClosedOI, OpenCI and InactivOC the drugs binding simultaneously all states with the same affinity, with higher affinity to the closed, to the open and to the inactivated state, respectively. We added the suffixes sss, ss, s, m, f and ff, depending on the slowest dissociation rate of the drug, which corresponded to 0.001, 0.003, 0.01, 0.1, 1 and 10 s^{-1}, respectively. Diffusion (k) and dissociation (r) rate constants for each drug-I_{Kr} interaction as tested in the model are included in the supplemental material (Tables S1 and S2). Drug doses ranging from $10^{-11.7}$ to $10^{-2.7}$ mol/L (M) with $10^{0.1}$ M steps were simulated for each virtual drug in order to

build their respective Hill plots. Temperature was set to 22ºC or 37ºC and intracellular and extracellular potassium concentrations were fixed to 130 and 4 mM, respectively.

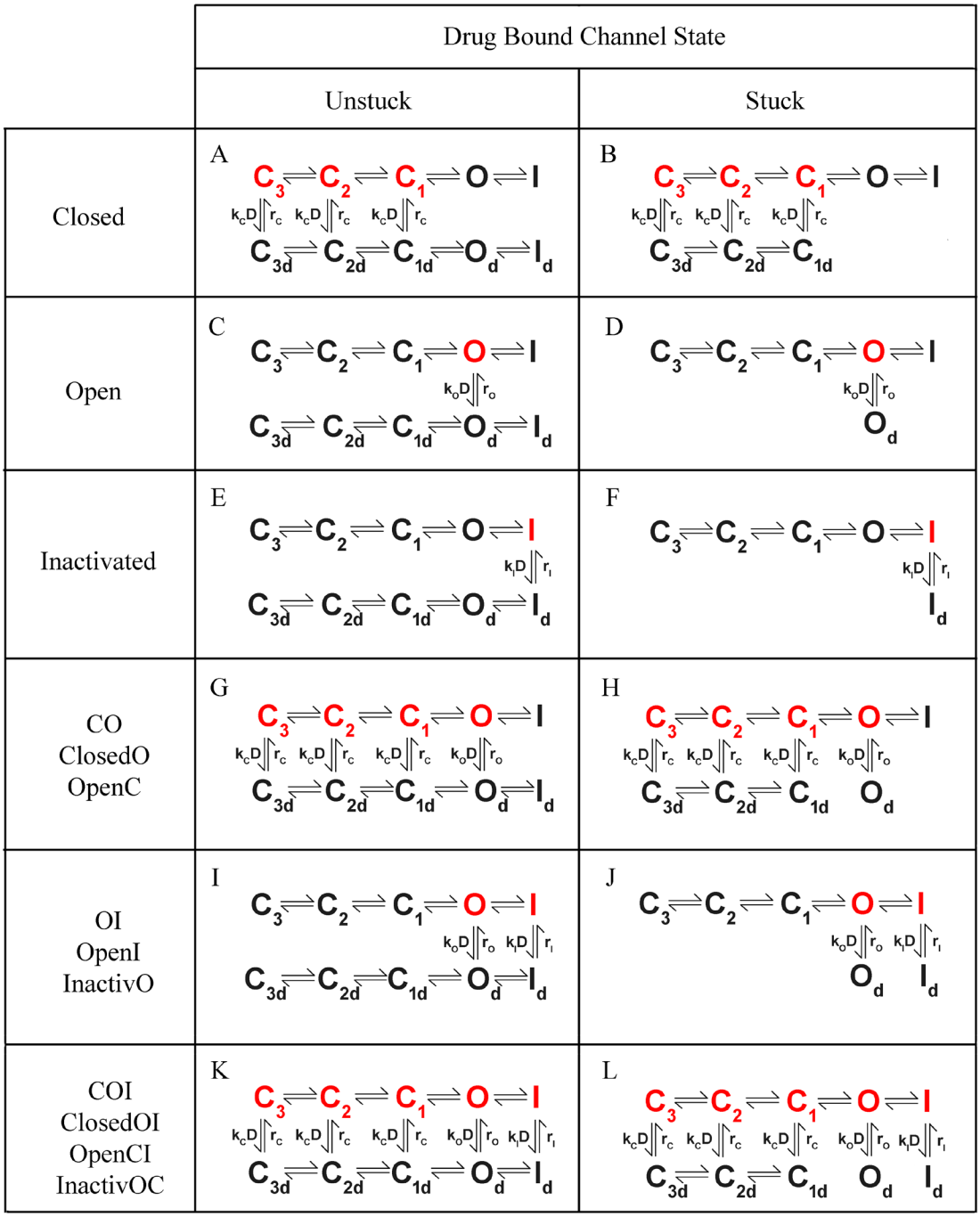

Figure 1. Simulated Markov drug-I_{Kr} interaction models with nondrug bound (C_3, C_2, C_1, O and I) and drug bound (C_{3d}, C_{2d}, C_{1d}, O_d and I_d) states considering unstuck (A, C, E, G, I and K) and stuck (B, D, F, H, J and L) drug bound channels. D is the drug concentration, and its product with

k_C, k_O and k_I corresponds to the association rates constants in the closed, open and inactivated states, respectively, and r_C, r_O and r_I are the dissociation rate constants in the closed, open and inactivated states, respectively. Binding states are red colored. First column indicates the corresponding type of drug-channel interaction and first row specifies the state of the channel when the drug is bound.

2.2 Simulation of the pseudo-ECG

Pseudo-ECGs were computed using a one-dimensional (1D) tissue model of a transmural wedge preparation, as in our previous work[21]. The 1D model was composed by 60 endocardial cells, 45 midmyocardial cells, and 60 epicardial cells, each cell being 100 μm long, as defined in O'Hara et al. model[22] and it was paced at 1 Hz. The propagation of the AP was described by the following nonlinear reaction diffusion equation:

$$C_m \frac{\partial V_m(x,t)}{\partial t} + \sum I_{ion} + \frac{a}{2}\frac{\partial}{\partial x}\left(\frac{1}{R_i(x)}\frac{\partial V_m(x,t)}{\partial x}\right) = 0$$

Where C_m stands for the membrane capacitance, a is the radius of the fiber, $\sum I_{ion}$ is the sum of all the ionic currents flowing through the cellular membrane and R_i represents the intracellular resistivity. Drug blocking effect on I_{Kr} was formulated using the standard sigmoid dose-response curve, parameterized using the half-maximal response dose (IC_{50}) and considering a Hill coefficient of 1 as in previous studies[21,23–26]:

$$\frac{I_{Kr}(D)}{I_{Kr}} = \frac{1}{1 + \frac{D}{IC_{50}}} = 1 - b$$

where D is the drug concentration and "1 – b" is the fraction of unblocked channels.

2.3 Experimental methods

All experiments were conducted manually with an EPC-10 amplifier (HEKA, Lambrecht/Pfalz, Germany) at room temperature in the whole-cell mode of the patch-clamp technique. HEK-293

cells stably expressing hKv11.1 (hERG) under G418 selection were a generous gift from Craig January (University of Wisconsin, Madison). Cells were cultured in DMEM containing fetal bovine serum 10%, glutamine 2 mM, Na+ pyruvate 1 mM, penicillin 100 U/L, streptomycin 171.94 µM (100 µg/ml), and G418 1 M (500 mg/ml). Before experiments, cells were lifted using TrypLE and plated onto poly-L-lysine–coated coverslips, Patch pipettes were pulled from soda lime glass (micro-hematocrit tubes) and had resistances of 2-4 MΩ. We used normal sodium Ringer for the external solution (in mM: NaCl 160, KCl 4.5, CaCl2 2, $MgCl_2$ 1, HEPES 10 (adjusted to pH 7.4, using HCl and NaOH, and 290–310 mOsm). The internal solution contained (in mM) $CaCl_2$ 5.375, $MgCl_2$ 1.75, EGTA 10, HEPES 10, KCl 120, NaATP 4 (adjusted to pH 7.2, using HCl and NaOH, and 300–320 mOsm). For all experiments, solutions of dofetilide and moxifloxacin were always freshly prepared from 1, 10 or 100 mM stock solutions in DMSO during the experiment. The final DMSO concentration never exceeded 1%.

2.4. Stimulation protocols

Three different sets of voltage clamp protocols were used. The first and third sets were designed in this work while the second was adopted from the literature. The first set was composed of our new stimulation voltage clamp protocols, which consisted of a 5-s variable voltage conditioning step (at -80 mV, 0 mV and 40 mV) followed by a 0.2-s test pulse at -60 mV repeated at 5.4-s intervals, from a holding potential of -80 mV (Figure 2, top). When the 5-s variable voltage was fixed at -80 mV, a 0.5-ms pre-pulse at 20 mV was included and the 0.2-s test pulse was applied at -50 mV. These protocols were called P-80, P0 and P40, respectively. The second set was composed of Protocol-O, Protocol-C and the standard protocol defined by Yao et al. 2005[5] (Figure 6C). Protocol-O consisted of a 4.8-s conditioning step at 20 mV followed by a 0.5-s test pulse at -50 mV repeated at 6-s intervals, from a holding potential of -80mV. Protocol-C consisted of a 1-s

conditioning step at 20 mV followed by a 5-s test pulse at -50 mV repeated at 60-s intervals, from a holding potential of -80 mV. The standard protocol consisted of a 4.8-s conditioning step at 20 mV followed by a 5-s test pulse at -50 mV repeated at 15-s intervals, from a holding potential of -80 mV. The third set of protocols consisted of two action potential clamp protocols, P_AP1 and P_AP2, which were generated using a version of the mid-myocardial O'Hara et al. AP model[22] whose I_{Kr} is reduced to 40% at 0.5 Hz and 2 Hz, respectively.

I_{Kr} and hERG channels were stimulated repeatedly until reaching the steady state at pretreatment control and under drug application. Peak tail currents amplitudes were measured at steady state and Hill plots were constructed by plotting the steady-state tail peak current normalized to control for each concentration versus the decimal logarithm of the drug concentration, as in previous studies[5,6,25,27].

3. Results

3.1 Design of voltage protocols

As drug-channel interaction may depend on the conformational state of the channel, and it depends on the membrane voltage, we studied the influence of the voltage of the conditioning step of the stimulation protocol on the probability of the I_{Kr} channel to occupy a specific conformational state using computer simulations. For this purpose, we considered a stimulation voltage clamp that consisted of a 5-s variable voltage (V_m) conditioning step followed by a 0.2-s test pulse at -60 mV repeated at 5.4-s intervals from a holding potential of -80 mV (Figure 2, top). This protocol was applied in control (absence of drug) at different conditioning step voltages. Then, the average of the probabilities of the three closed states (C_{AVG}, solid line), the open state (O_{AVG}, dashed line) and the inactivated state (I_{AVG}, dotted line) for the whole protocol duration were computed as a function of the conditioning step voltage (Figure 2A). Moreover, the differences C_{AVG} - O_{AVG} (Figure 2B)

and I_{AVG} - O_{AVG} (Figure 2C) were also calculated, as these differences will be key to select the conditioning step voltages that will provide more information about the blocking potency of the drug. Indeed, unstuck OpenC drugs are expected to produce the highest block when the stimulation protocol is such that maximizes the probability of the open state (close to 0 mV, Figure 2A, long dashed line) while the probability of the closed state is low. It would occur when the C_{AVG} - O_{AVG} is small and O_{AVG} is relatively high, which would correspond to a conditioning pulse close to 0 mV (Figure 2B). In addition, the lowest inhibition of the channels would occur when the C_{AVG} - O_{AVG} is maximum, which takes place for conditioning pulses at low voltages (Figure 2B). Therefore, the maximum and minimum IC_{50} of unstuck OpenC will be expected when applying this protocol with conditioning pulses close to -80 mV and 0 mV, respectively. For conditioning pulses at higher voltages, such as 40 mV the IC_{50} would be expected to be closer to the value obtained with the conditioning pulse at 0 mV. In the case of unstuck ClosedO drugs, the opposite behavior is expected. Regarding drugs with different affinities to the open and inactivated states, as I_{AVG} - O_{AVG} is maximum at 40 mV (Figure 2C), adoption of this voltage for the conditioning pulse would yield high inhibition for unstuck InactivO drugs. Therefore, application of this protocol with conditioning steps at -80 mV, 0 mV and 40 mV would highlight the differences in the potency of block with the voltage. As conditioning steps at -80 mV raised very small currents to be measured in the experiments, we modified this protocol to include a pre-pulse at 20 mV for 0.5 s to open the channels. These protocols were labelled P-80, P0 and P40, respectively, as indicated in the methods section. Figure 3A shows a representation of each protocol.

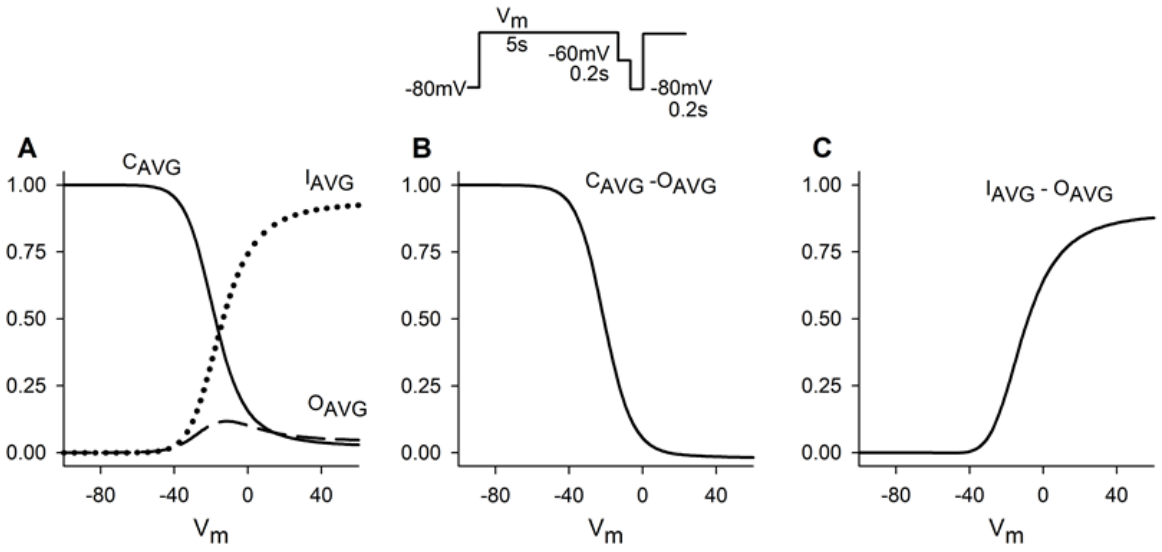

Figure 2. Simulated influence of the voltage of the stimulation protocol on the probabilities of the states of the I_{Kr} channel at 22ºC. Stimulation protocol (top), averages (A) of the simulated probabilities of the closed states (C_{AVG}, solid line), the open state (O_{AVG}, dashed line) and the inactivated state (I_{AVG}, dotted line) for the whole protocol duration as a function of the voltage of the conditioning step (V_m) and the difference between the average of the simulated probabilities of the closed states and the open estate (C_{AVG} - O_{AVG}, B) and the difference between the average of the probabilities of the inactivated state and the open estate (I_{AVG} - O_{AVG}, C).

3.2 Simulated effects of voltage protocol on the IC_{50}

Once the stimulation protocols were designed, I_{Kr} inhibition produced by all the prototypical drugs was examined using P-80, P0 and P40.

Figure 3 summarizes the results obtained for three selected drugs: unstuck Inactivated_s (Figure 3B), stuck Inactivated_s (Figure 3C) and stuck ClosedO_s (Figure 3D). The voltage clamp protocols are represented at the top panel (Figure 3A). The Markovian schemes of the simulated drug-I_{Kr} interactions are illustrated in the first column, the steady state currents traces elicited for

each protocol, namely, P-80, P0 and P40, are depicted in the second, third and fourth column, respectively, and the corresponding Hill plots are constructed in the last column. Unstuck Inactivated_s (Figure 3B) produced similar inhibition of I_{Kr} tail currents with P-80, P0 and P40, so the resulting Hill plot curves are superimposed and the IC_{50}s values are the same. Indeed, in the case of unstuck drugs that only bind and unbind to one state, the IC_{50} values do not depend on the stimulation protocol, as it is determined by the ratio between the diffusion (k) and the "off" rate (r). Although the steady state block is the same for each protocol, the time needed to reach it depends on the voltage protocol as it determines the mean probabilities of the channel of being on each state, and, therefore the average of the time during the cycle to be on the state where the drug can bind and unbind. However, stuck Inactivated_s (Figure 3C) had higher inhibitory effects with protocols P0 (second column) and P40 (third column) than with P-80 (first column), which is consistent with the fact that I_{AVG} is high for P0 and P40 and almost zero for P-80 (Figure 2A, V_m = 0, 40 and -80 mV, respectively). For example, 10 nM stuck Inactivated_s inhibited tail currents by approximately 50% with P0 and P40, whereas it only reached approximately 20% with P-80. Subsequently, the Hill plot curves and the IC_{50} values corresponding to P0 (red) and P40 (green) are similar while the one corresponding to P-80 (blue) is shifted to the left. Therefore, Hill plots of drugs binding just to one state of the channel were highly dependent on the state of the drug bound channel. Unstuck variants had the same IC_{50} with the three protocols while the stuck ones exhibited the smallest IC_{50} with the protocol that enhanced the probability of the state where the drug binds and unbinds; P40, P0 and P-80 for Inactivated (Figure 3C), Open and Closed drugs, respectively (not shown). Finally, stuck ClosedO_s (Figure 3D) revealed higher potency to block I_{Kr} with P-80, followed by P0, than with P40, so the Hill plot curves as well as the IC_{50} values are different. It is in close agreement with the inverse dependency of C_{AVG} and $C_{AVG} - O_{AVG}$ with V_m

(Figures 2A and 2B). These results indicate that unstuck Inactivated_s (Figure 3B) produces voltage independent I_{Kr} steady-state block. On the contrary, stuck Inactivated_s (Figure 3C) produces smaller I_{Kr} inhibition at low voltages, as it binds and unbinds to the inactivated state, and stuck ClosedO_s (Figure 3D) at high voltages, as it has a preferential affinity to the closed states. Therefore, the dissimilar effects produced by the drugs when applying our set of voltage clamp protocols manifest the differences in drug-channel interactions.

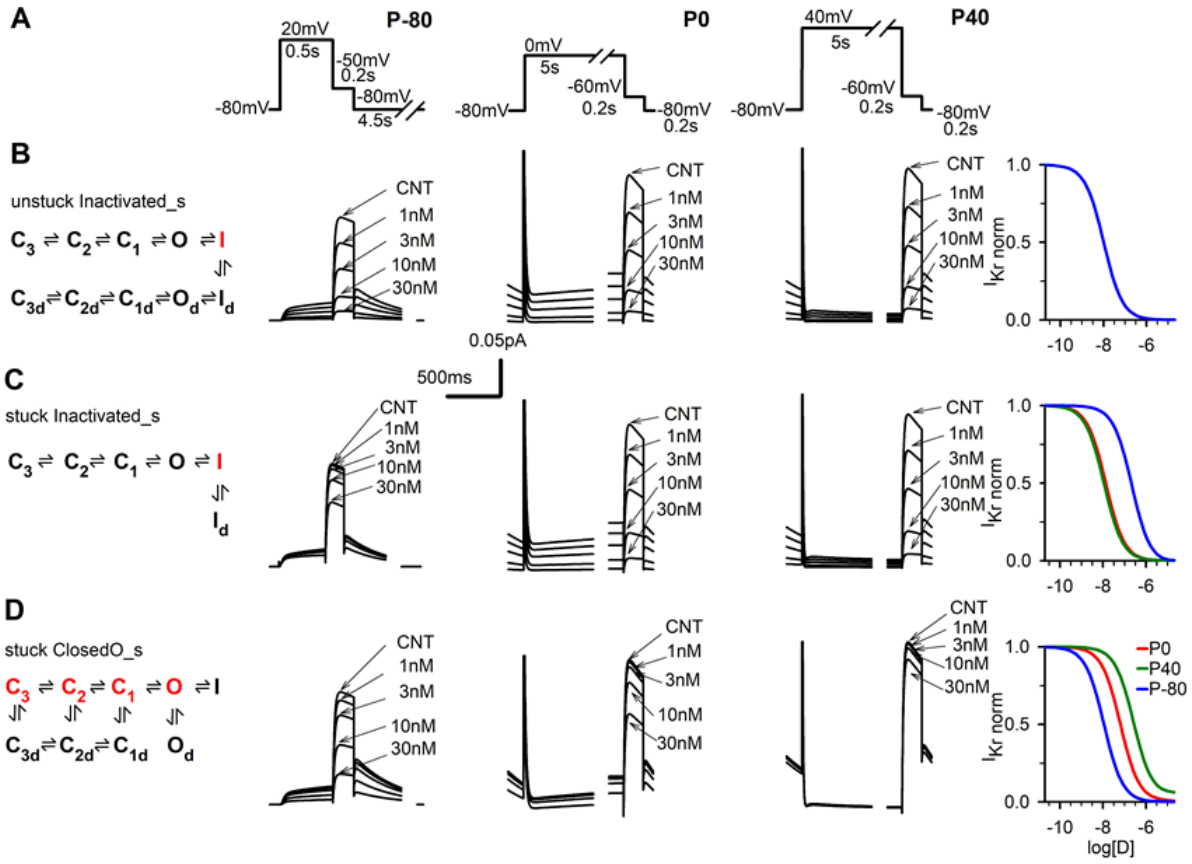

Figure 3. Simulated effects of voltage clamp protocols on IC_{50}. Voltage clamp protocols (A) and the corresponding steady state current traces before and after the application of selected virtual drugs: unstuck Inactivated_s (B), stuck Inactivated_s (C) and stuck ClosedO_s (D) at 22 ºC. First

column represents the Markovian schemes of the simulated drug-I_{Kr} interactions. Second, third and fourth columns correspond to the steady state currents traces elicited for each protocol and arrows indicate peak tail current amplitudes at marked concentrations. Last column illustrates the corresponding Hill plots.

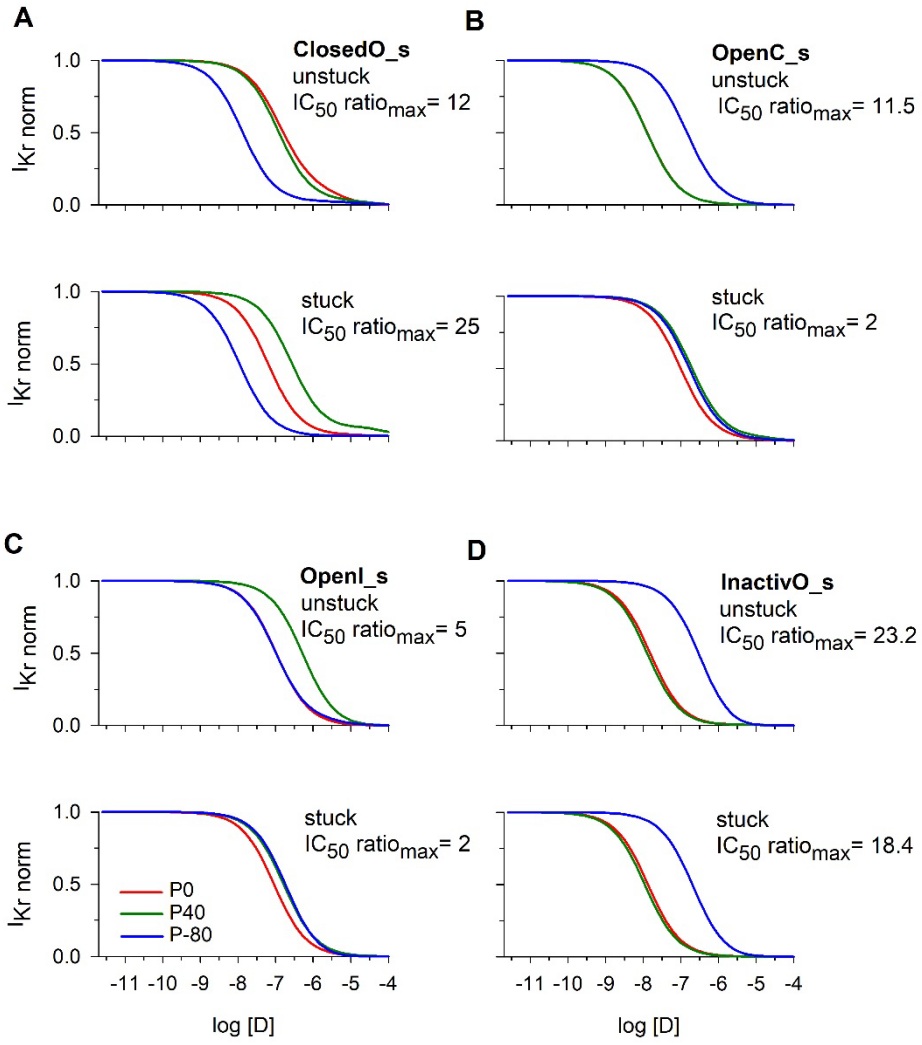

Figure 4. Simulated Hill plots for each type of the prototypical drugs binding to two states with state-dependent affinities using the proposed protocols: P-80 (blue), P0 (red) and P40 (green) at 22ºC. Unstuck (top) and stuck (bottom) variants of ClosedO_s (A), OpenC_s (B), OpenI_s (C) and InactivO_s (D). The maximum IC_{50} ratio for each drug is also indicated in each panel.

Figure 4 illustrates the simulated Hill plots for each type of the prototypical drugs binding to two states with state-dependent affinities using the proposed protocols: P-80 (blue), P0 (red) and P40 (green) at 22ºC. Both variants of ClosedO_s (Figure 4A) have the minimum IC_{50} with P-80, as expected, as more channels are closed at -80 mV, while the maximum IC_{50} is registered with P0 or P40. In the case of OpenC_s drugs, the maximum IC_{50} is registered with P-80, which maximizes the time the channels are closed and tends to reveal the drug's affinity to this state. OpenI_s drugs only showed small differences of IC_{50}, P0 being the protocol showing the smallest IC_{50}, as it is the one that enhances the most the probability of the open estate. In the case of unstuck OpenI_s, the IC_{50} obtained with P-80 is very similar to the one corresponding to P0. It could be due to the pre-pulse delivered at 20 mV for 0.5 s to open the channels before the test pulse. Finally, the maximum IC_{50} of InactivO_s (Figure 4D) is registered with P-80 as this protocol minimizes the probability of the inactivated state, when the affinity of the drug is higher. Drugs with similar state preferences and drug bound states exhibited similar Hill plot patterns although the maximum IC_{50} ratio depended on the value of the slowest dissociation rate of the drug. For example, the maximum IC_{50} of InactivO_m also corresponded to P-80 and the IC_{50}s obtained with P0 and P40 were very similar, like InactivO_s. However, the maximum IC_{50} ratio was 13.0 instead of 23.2, which was the corresponding to InactivO_s (Figure 4D). These results suggest that the influence of the voltage clamp protocol on the estimation of the inhibitory effects of a compound depends on the specific interaction with the channel.

As this study was extended to the 144 *in silico* drugs, Hill plots for every prototypical drug were constructed using our proposed protocols (P0, P40 and P-80) and IC_{50} values were extracted. Figure 5 summarizes the maximum IC_{50} ratios for each drug-channel interaction. Unstuck and stuck variants are represented with non-filled and filled bars, respectively. The highest IC_{50} ratios

were observed for the stuck variants of Closed, ClosedO and ClosedOI drugs, and some unstuck variants of InactivOC, InactivO, ClosedO, ClosedOI and OpenC drugs. The highest, mean and median values of the maximum IC_{50} ratio were 51.2, 8.7 and 2.7, respectively. Moreover, 13.9 % of the prototypical drugs exhibited a ratio above 20-fold and the 34% yielded a ratio above 10-fold. On the contrary, unstuck drugs binding and unbinding to one state (Closed, Open and Inactivated), two states (CO and IO) or all states with the same affinity (COI) exhibited voltage independent IC_{50}s. IC_{50}s of stuck drugs whose preferential state for binding and unbinding are the open state (Open, OpenC, OpenI and OpenCI) showed a very small dependence on the voltage protocol, followed by the unstuck variant of Open_I and both unstuck and stuck variants of InactivO_f, InactivO_ff and OpenC_ff. Stuck drugs tended to register higher IC_{50} ratios than unstuck drugs, the mean maximum IC_{50} ratio for stuck drugs being 11.2 while for unstuck drugs being 6.2. However, most unstuck variants of OpenC, OpenI and InactivO displayed higher IC_{50} ratios than the corresponding stuck variants. Finally, the speed of the association and dissociation rates played a relevant role, although their effects were highly drug-dependent. For example, fast rates tended to increase the maximum IC_{50} ratio in stuck drugs binding and unbinding to the closed state. By contrast, fast dynamics decreased this ratio in drugs binding simultaneously to both the inactivated and open states with higher affinity to the inactivated state.

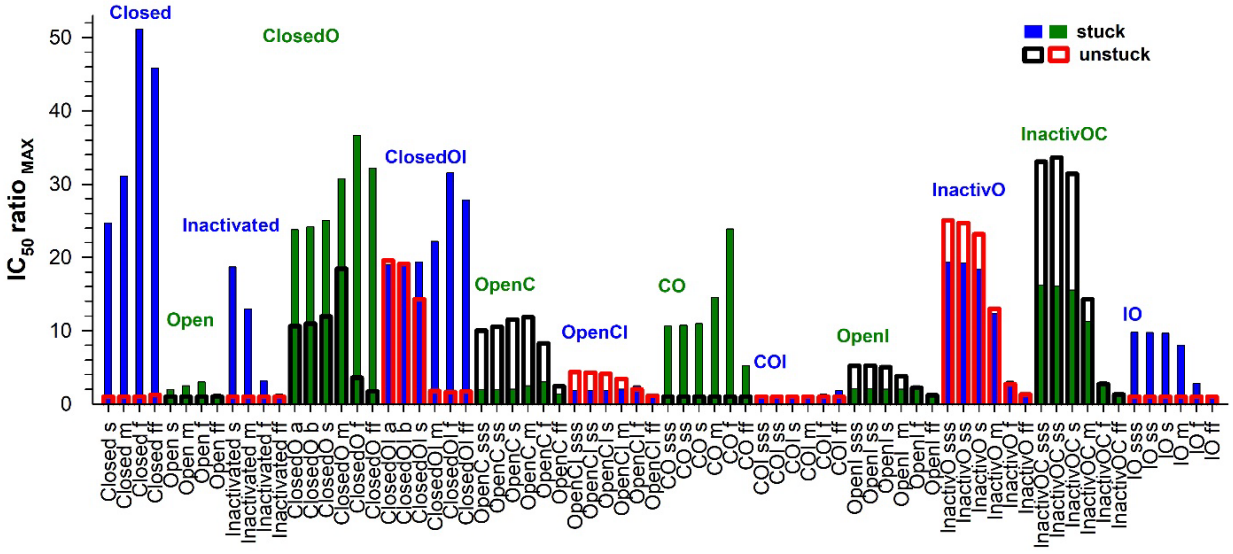

Figure 5. Maximum IC_{50} ratios obtained with our proposed protocols (P0, P40 and P-80) at 22ºC. Filled (blue and green) and non-filled (black and red) bars for stuck and unstuck drugs, respectively.

I_{Kr} inhibition produced by all the prototypical drugs was also simulated using the Protocol-O, Protocol-C and the standard protocol experimentally used by Yao, et al. 2005[5] (Figure 6C). Figure 6 shows the simulated Hill plots of stuck ClosedO_f obtained with ours (A) and Yao and colleagues' ones (B). In this case, our protocols provided a maximum IC_{50} ratio of 51.5 while Yao and coworkers' ones yielded 37.6. Maximum IC_{50} ratios obtained with both sets of protocols for all prototypical drugs are provided in the supplemental material (Figure S1). Maximum, mean and median values of the maximum IC_{50} ratios obtained with Yao and coworkers' protocols were 37.7, 6.5 and 3.1, respectively, which are smaller than those registered with ours (51.2, 8.7 and 2.7, respectively). Therefore, our new protocols could be more useful than those currently available in the literature to detect those compounds that obstruct the channel to a different extent depending on the stimulation voltage.

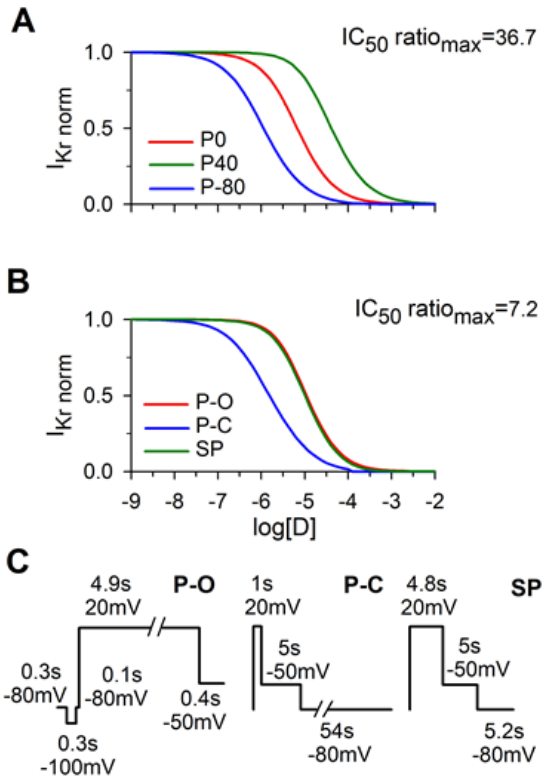

Figure 6. Simulated Hill plots for stuck ClosedO_f using our proposed protocols (A) and with Yao, Du, et al. (2005) protocols (B) at 22ºC. A: P0 (red), P40 (green) and P-80 (blue). B: Protocol-O (P-O, red), Protocol-C (P-C, blue) and standard protocol (SP, green). C: Yao et al. voltage clamp protocols[5]. The maximum IC_{50} ratio for each drug is also indicated in each panel.

Our protocols were also used to simulate Hill plots for every prototypical drug at 35ºC. Although the effects of temperature on binding and unbinding rates of the virtual drugs was not included, our results were temperature-dependent as the formulation of the transition rates between the channel states was temperature-dependent. Absolute and relative to 22ºC maximum IC_{50} ratios at 35ºC are provided in the supplemental material (Figure S2). Maximum IC_{50} ratios at 35ºC exhibited a similar tendency to those at 22ºC although important differences were observed. The highest IC_{50} ratio at 35ºC was 105.1. The maximum IC_{50} ratio that increased the most with temperature belonged to unstuck ClosedO_s (Figure 7A) while the one that decreased the most

corresponded to stuck InactivO_sss (Figure 7B). Temperature-related differences for the other virtual drugs were smaller than two-fold. Therefore, the impact of voltage protocol on the IC_{50} is influenced by temperature, although to a small extent.

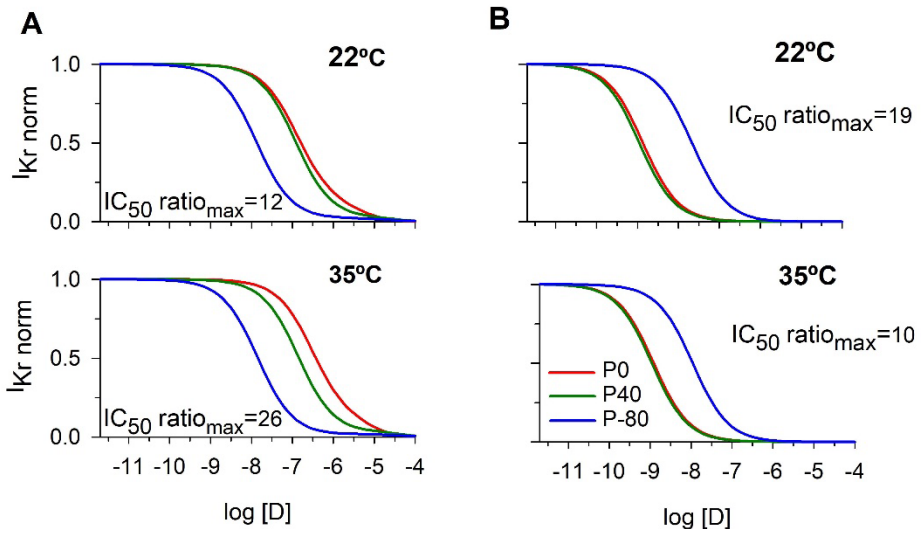

Figure 7. Simulated Hill plots for unstuck ClosedO_s (A) and stuck InactivO_sss (B) using the new protocols at 22ºC (top) and 35ºC (bottom). The maximum IC_{50} ratio for each drug is also indicated in each panel.

3.3 Experimental validation

In order to provide an experimental validation to our results, our protocols were applied to construct the experimental Hill plots of two well-known I_{Kr} blockers, moxifloxacin and dofetilide, at 22ºC. The moxifloxacin IC_{50} corresponding to P0, P40 and P-80 was 373, 196 and 143 μM, respectively (Figure 8A, left panel), which gives rise to a maximum ratio of 2.6. This ratio is in accordance to the experiments of Alexandrou et al. 2006[28] performed at 22ºC, that provide a maximum ratio of 1.9. A much more dilated influence of the stimulation protocol on dofetilide IC_{50} was registered. Hill plots look completely different (Figure 8B, left panel) and disparate IC_{50} values are obtained: 57, 193 and 695 nM, which correspond to P0, P40 and P-80, respectively. It

yields a maximum ratio of 12.2, which is approximately 3-fold the one calculated from studies where the only factor that changed was the voltage protocol[12]. Moreover, our experiments support our finding that no stimulation protocol can provide the maximum IC_{50} for every drug. Indeed, P-80 protocol raised the maximum moxifloxacin IC_{50} value while P0 provided the minimum, contrarily to dofetilide.

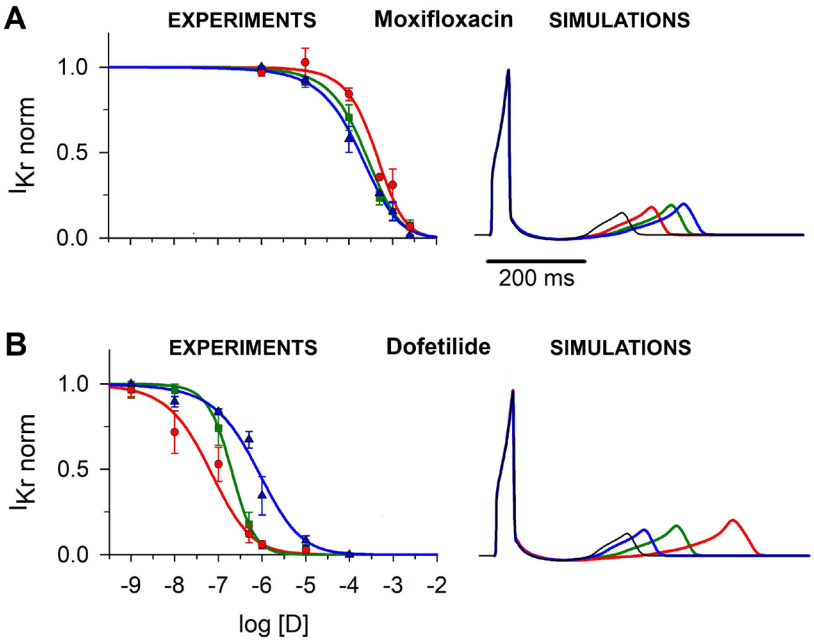

Figure 8. Experimental Hill plots (left column) and simulated steady state AP of isolated endocardial cells (right columns) for moxifloxacin (top row) and dofetilide (bottom row). Hill plots were obtained using the proposed protocols: P-80 (blue), P0 (red) and P40 (green). Symbols and vertical bars are presented as mean±S.E.M. (n=4 for all data points). An extra sum-of-squares F test with alpha set to 0.05 (GraphPad Prism5; GraphPad Software, La Jolla, CA) was performed to compare the curves to each other (moxifloxacin: P40 vs P0 $p = 0.0013$, P40 vs P-80 $p = 0.1646$, P0 vs P-80 $p < 0.0001$ and dofetilide: P40 vs P0 $p = 0.0003$, P40 vs P-80 $p < 0.0001$, P0 vs P-80 $p < 0.0001$). Simulated steady state pseudo-ECG in control (black) and in the presence of 196 µM

of moxifloxacin and 193 nM of dofetilide considering the IC_{50} obtained using the P-80 (blue), P0 (red) and P40 (green).

Therefore, our experiments support the potential use of our protocols to discriminate drugs with a small protocol dependence of drug block, like moxifloxacin, from drugs with an enormous dependence, like dofetilide. Our experiments also corroborate that the maximum IC_{50} ratios obtained with our protocols are higher than with previous protocols, and the difficulty to define a unique protocol to assess the I_{Kr} IC_{50} for all I_{Kr} blockers.

3.4 Simulated effects of IC_{50} differences on the QT interval

In order to show how dissimilar estimates for the IC_{50} would affect the prediction of drug-induced QT interval prolongation, pseudo-ECGs were computed in the presence of moxifloxacin and dofetilide. Concentrations of both drugs were fixed to the IC_{50} values obtained with P40, as this protocol provided an intermediate IC_{50} value for both drugs. Then, drug block was simulated using the simple pore equation without considering the kinetics and conformational state preference, as done in many previous works[21,23–25]. Figure 8A and 8B show that when the estimate of the IC_{50} used in the simulations was the one obtained with P40, a 106 ms QT prolongation - from 310 ms in control (black) to 416 ms (green) - was predicted in both cases, as 50% of the channels are closed. However, different QT prolongations were observed when considering the IC_{50} estimates obtained with P-80 (blue) and P0 (red). The discrepancies were higher for dofetilide (242 versus 34 ms, bottom row) than for moxifloxacin (134 versus 60 ms, top row), as estimates of IC_{50} were more disparate. We also simulated the pseudo-ECGs in the presence of the following therapeutic concentrations: 6.23 μM moxifloxacin and 2 nM dofetilide (see Figure S3 in the supplemental material). The predicted QT intervals for moxifloxacin were 318, 319 and 323 ms when using the IC_{50}s corresponding to P40, P0 and P-80, respectively, and for dofetilide they were

326, 322, and 317 ms, respectively. Again, the discrepancies were higher for dofetilide (9 ms) than for moxifloxacin (5 ms). Therefore, differences in estimates for the IC_{50} involve variances in the prediction of QT interval.

3.6 Clinical relevance of the IC_{50} s obtained with the proposed stimulation protocols

The ultimate objective of studying the blocking potency of drugs is to know the effects of the drugs *in vivo*. As our proposed stimulation protocols are far from the time courses of the membrane potentials *in vivo*, we also aimed to investigate the drug effects when stimulating the channels with AP waveforms to study whether the blocking effects observed with our three proposed protocols are close to those estimated with more realistic voltage waveforms. For this purpose, we simulated the Hill plots for every prototypical drug with P_ AP1 and P_ AP2, which correspond to the steady state APs obtained using a version of the mid-myocardial O'Hara et al. AP model[22] whose I_{Kr} is reduced to 40% at 0.5 Hz and 2 Hz, respectively. Figure 9 illustrates these AP clamp protocols (A and B) and shows a comparison of the simulated Hill plots with these AP clamps (dotted) and with our three proposed protocols (solid) for each type of the prototypical drugs binding to two states with state-dependent affinities. Our results showed that the curves obtained with P_AP1 were similar to the ones corresponding to P80 while those registered with P_AP2 looked like those obtained with P0. This observation seems reasonable as in P_AP1 the membrane voltage is -80 mV most of the time with short intervals of positive potential and in P_AP2 the membrane voltage is close to 0 mV for a long proportion of the time. These results may lead to the conclusion that P-80 and P0 would be enough to characterize I_{Kr} block under realistic conditions, P40 being less relevant. However, the IC_{50} obtained with P40 could be useful to study I_{Kr} block in situations that promote channel inactivation. Our results suggest that the blocking potencies observed with our

three proposed protocols are in line with the ones that will be exerted under realistic voltage waveforms.

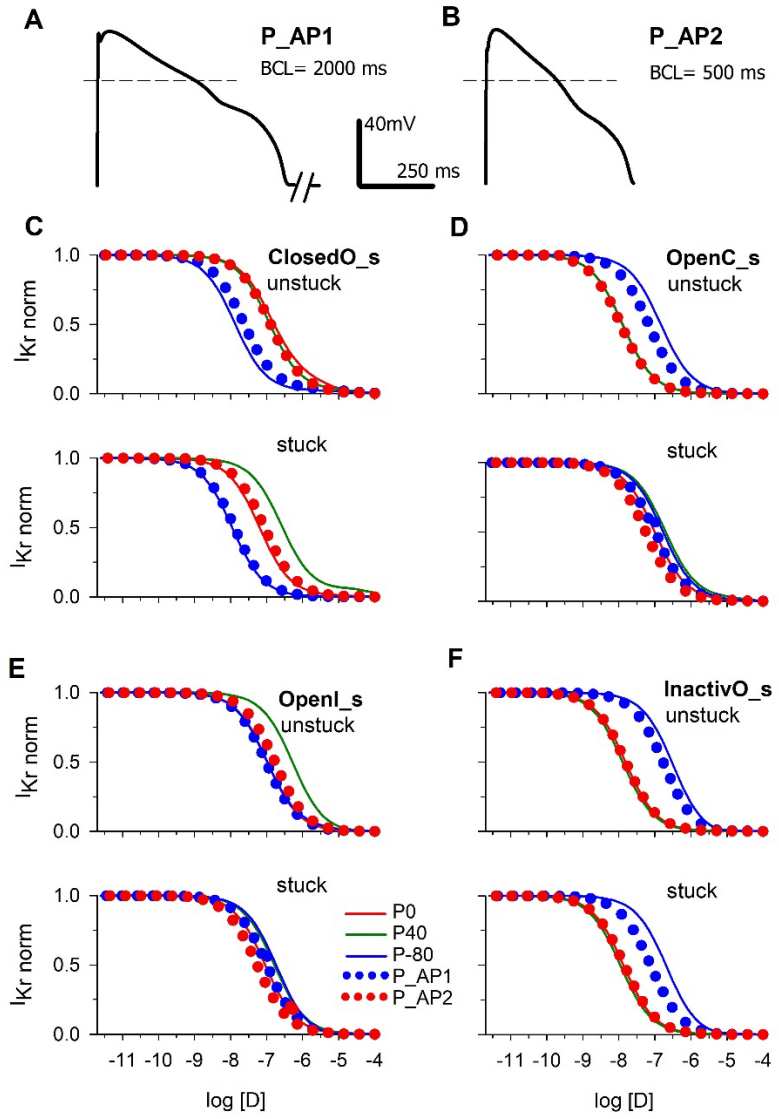

Figure 9. Comparison of the simulated Hill plots obtained with two action potential clamp protocols, P_AP1 (dotted blue) and P_AP2 (dotted red), which are illustrated in (A) and (B), and with our proposed protocols: P-80 (solid blue), P0 (solid red) and P40 (solid green), at 22ºC. Each type of the prototypical drugs binding to two states with state-dependent affinities are represented:

unstuck (top) and stuck (bottom) variants of ClosedO_s (C), OpenC_s (D), OpenI_s (E) and InactivO_s (F).

4. Discussion

4.1 Main findings

We developed a computational approach to investigate whether the IC_{50} values obtained for a certain drug could be good estimators of the inhibitory effects *in vivo* and to propose improvements in the assessment of the blocking potency. Firstly, we designed new experimental stimulation protocols to detect different inhibitory potencies depending on the voltage. Secondly, we simulated a wide variety of I_{Kr}–drug interactions with increasing drug concentrations using the new stimulation protocols. Thirdly, we extracted the IC_{50} values for each drug with the new protocols and with others from the literature and calculated the maximum ratio of IC_{50} for each drug-protocol combination. Fourthly, we performed experiments to support our theoretical observations. Finally, we investigated the drug effects when stimulating the channels with realistic AP waveforms at different frequencies and they were in line with the effects observed with our three new protocols.

Our results revealed that our proposed three-protocol IC_{50} assay improves the assessment of the blocking potency of drugs and can be very useful to decide whether the IC_{50} values accurately assess the inhibitory effects of the drug *in vivo*. Our results suggest that when the IC_{50} values resulting from applying our three protocols to a compound are similar, then, the IC_{50} could be a good indicator, otherwise kinetics and preferential state biding properties should be taken into account to predict the blocking potency of the drug *in vivo*. Our results revealed a much more pronounced impact of the stimulation protocol on the IC_{50} than previous experimental studies. Indeed, the mean and the highest value of the maximum ratio of IC_{50} were 8.9 and 105.1, respectively, much higher than 4.3 and 10.3, the corresponding values calculated from

experimental studies where the voltage protocol was the only factor that changed[5]. Our experiments also support that our protocols may yield higher IC_{50} differences than other protocols available in the literature. This can be due to two important aspects. First, our protocols were specifically designed to unmask the potential differences in the blocking effects of a compound due to the existence of dissimilarities in the affinities to each conformational state of the hERG channel. And second, the generation and simulation of a wide variety of dynamic models of I_{Kr}-drug interaction with very diverse kinetics and affinities to the conformational states of the channel, which is to date hardly possible to achieve experimentally. Importantly, our experiments confirmed that the protocol providing the maximum IC_{50} value was drug-specific. This suggests that adoption of a standard stimulation protocol would dramatically underestimate or overestimate the blocking potency of certain drugs. In our opinion, the use of our three proposed protocols is crucial to build a better picture of the inhibitory effects and the possible clinical outcomes of a compound.

4.2 Impact of the stimulation protocol on blocking potency estimation

Some experimental studies have evidenced that the blocking potencies of drugs may vary with the stimulus pattern. Kirsch, et al. 2004[4] used several patch-clamp voltage protocols to study hERG inhibition of 15 drugs. They found differences in the IC_{50} for some drugs, the maximum IC_{50} ratio being 3.2. Later, Yao, et al. 2005[5] designed two voltage protocols, Protocol-O and Protocol-C, and compared their results with the standard protocol. BeKm-1, a compound that preferentially block the channel in the closed, showed the biggest differences in the concentration-response curves. This is in agreement with our simulations, as most of the highest IC_{50} ratios correspond to virtual drugs that exclusively or preferentially bind in the closed state (see Figure 5). However, the IC_{50} ratios obtained for these drugs in our simulations are higher than 20 (up to 105.1) while the ratio

registered for BeKm-1 is 10.3. It corresponds to the ratio between the IC_{50} obtained with a standard protocol over the IC_{50} obtained with Protocol-O. Protocol-C revealed smaller block but, unfortunately, the concentration-response curve was incomplete and no IC_{50} was provided. Obtention of the full curve could have provided a higher IC_{50} ratio.

More recently, Milnes et al. 2010[12] studied the effects of the stimulation protocol on hERG inhibition for cisapride and dofetilide at 37ºC. They provided a maximum IC_{50} ratio of 10.3 and 3.75, respectively, when only changing the voltage protocol. The maximum ratio in our experiments with dofetilide is 12.8, which is higher than 3.75. This can be due to the differences on the stimulation protocols and temperature.

Our results also reveal that protocols yielding the maximum IC_{50} and minimum IC_{50} depend on the drug. Our experiments provided the lowest IC_{50} value with P-80 in the case of moxifloxacin and with P0 for dofetilide. Our observation that the protocol revealing the maximum potency of block is drug-dependent is also supported by Yao et al. 2005[5].

Therefore, our study of the impact of the stimulation protocol on the estimation of current inhibition is in accordance with previous experiments, but it reveals a more critical role of the voltage protocol. A very recent investigation has studied protocol-dependent differences in IC_{50} and observed that state preferential binding, drug-binding kinetics and trapping are key factors[13]. Their Markov models included state-dependent block, but they did not reproduce other important characteristics, like closed-state trapping[13]. Contrarily, our Markovian models are very comprehensive as they reproduce state-dependent block, trapping as well as drug binding and unbinding to any state of the channels. Moreover, our models can mimic drug bound channels changing its conformational state or remaining unchanged.

In order to know if our main results were highly dependent on the ionic channel model, we repeated some key simulations using two additional formulations of hERG channel: Lee et al.[19] and Li et al.[29] models. These two Markovian models have distinct structures and transition rates, which are also different from Fink et al. model. Figures S4 and S5 of the supplemental material represent the Markovian schemes (left column) and the simulated Hill plots for each type of the prototypical drugs binding to two states with state-dependent affinities using the proposed protocols: P-80 (blue), P0 (red) and P40 (green) at 22ºC using Lee et al. and Li et al. hERG models, respectively. These figures show the simulated Hill plots for each type of the prototypical drugs binding to two states with state-dependent affinities using the proposed protocols, as in Figure 4, where they were simulated using Fink et al model[16]. The patterns of the Hill plots obtained with the three models were very similar, although there are quantitative differences that affect the values of the maximum IC_{50} ratios. In the three cases, the IC_{50} protocol dependency relied on the tested compounds and the protocols yielding the maximum IC_{50} and minimum IC_{50} depended on the drug with the three ionic models. Indeed, both variants of ClosedO_s (Figures 4A, S4B and S5B) have the minimum IC_{50} with P-80 and the IC_{50} registered with P0 and P40 are substantially higher. Also, in the case of OpenC_s drugs (Figures 4B, S4C and S5C), the maximum IC_{50} was registered with P-80 and the minimum with P0, which is similar to the one obtained with P40. In addition, OpenI_s drugs showed small differences of IC_{50} with the three models (Figures 4C, S4E and S5E), the minimum IC_{50} being obtained with P0, although it could be very similar to the ones registered with the other protocols. Moreover, the maximum IC_{50} of InactivO_s was registered with P-80 with the three models (Figures 4D, S4F and S5F) and the IC_{50} values obtained with P0 and P40 were similar. We have also obtained the Hill plots of unstuck and stuck Inactivated_s with Lee et al. and Li et al. models (see middle and bottom rows of Figure S6 of the supplemental material) and they

clearly resemble the ones obtained with Fink et al. model (top row of Figure S6 and right panels of Figures 3B and 3C), the unstuck variant having the same IC_{50} for the three protocols. Therefore, there are also drugs that showed no differences or small differences on the IC_{50} value when simulated with Lee et al. and Li et al. models. Overall, the main conclusions of this work hold when the ionic channel model is simulated with Lee et al. or the Li et al. models, which have different structures and transition rates from Fink et al. model.

4.3 Implications for drug safety assessment

Our work has important implications for drug safety assessment. Indeed, one of the most relevant cardiac safety tests of pharmacological compounds consists on the measurement of hERG IC_{50} *in vitro*[2]. As previously explained, other authors have shown differences on IC_{50} values, but they were smaller than in our work, and some of these authors considered that the use of a certain protocol could be enough for safety studies[4,5]. However, different protocols and temperatures are proposed. Kirsch and coworkers propose a step-ramp protocol at near-physiological temperatures[4], while Yao and colleagues propose the long pulse step protocol at room temperature[5]. More recently, the Comprehensive In vitro Proarrhythmia Assay (CiPA) initiative, led by the FDA, has raised the need of a standardization of the experiments used to obtain the IC_{50} values[30]. However, our results suggest that the existence of a wide variety of drug-channel interactions impairs the definition of a "standard" protocol to minimize the influence of the stimulation protocol on the IC_{50} measurement. In order to improve the assessment of drug safety, we suggest the adoption of a three-protocol IC_{50} assay. Provided that the differences in IC_{50} for a compound are small enough, the IC_{50} could be used for the assessment of the inhibitory effects of the compound. On the contrary, supposing the IC_{50}s resulted in very different values, the IC_{50} would be a poor indicator.

Then, other characteristics, like kinetics and state-dependent binding properties should be investigated to have a better picture of the blocking effects of the compound.

Although the proposed protocols do not correspond to electrophysiological conditions, our simulations with the action potential clamp protocols have shown that the Hill plots obtained with P-80 are close to those obtained with P_AP1 and P0 with P_AP2 which come from voltage membrane time courses of cells with reduced repolarization reserve at slow and fast pacing, respectively. Therefore, the IC_{50}s obtained from our protocols would be related to the blocking potencies of the drugs *in vivo*. However, considering only these two IC_{50} values would be an oversimplification, as electrical activity is very different during arrhythmic episodes or in the presence of pathologies, like hypo or hyperkalemia, ischemia, or heart failure. In addition, the AP waveform is not uniform in the heart. There are apico-basal and transmural differences. Purkinje AP time courses are also different from ventricular AP time courses and there is a natural intersubject variability. These reasons led us to try to design protocols to infer the drug potency in each conformational state of the channel. We designed P-80, P0 and P40 to investigate drug block in the closed, open and inactivated states, respectively. Although at 0 mV not all channels are open, the open probability is relatively high at that voltage. If the IC_{50}s obtained with the three protocols are similar, we can assume that the channel block that can occur in any real situation will be similar. On the contrary, if the values are disparate, the channel block produced by the drug may be extremely dependent on the situation.

Recent works propose alternative methods to assess the proarrhythmic risk of drugs by using the modeling and simulation of drug-channel interactions and considering the kinetics of block[31–33]. Some authors have even attempted to implement a standardized protocol for measurement of kinetics and potency of hERG block. Unfortunately, their results highlight the challenges in

identifying it over a range of kinetics[34]. We also agree that drug safety assessment would improve by considering the kinetics of block, but, to the best of our knowledge, most pharmaceutical companies are not constructing mathematical models of drug-hERG interactions based on current block measured using a dynamic voltage protocol, which seems to require a substantial time. Formulation of mathematical models describing drug channel interactions is not an easy work. Even the authors proposing this method obtain different models depending on the seed used to fit the model[32], which may lead to different predictions. In addition, drugs may bind and unbind the channel by many mechanisms and, as far as we are concerned, only a few possible types of drug-channel interactions are being accounted for in these attempts. Indeed, their Markovian models do not consider the possibility of the drug binding and unbinding to any channel state and their simulated drug bound channels have less conformational states than the unbound channels. Therefore, only a few types of drug-channel interactions are considered in these attempts. The above mentioned restrictions reduce the number of parameters to be fitted in the process of drug model development and simplify it. However, it can also lead to a misunderstanding of the mechanism of drug-channel interaction, which can result in unrealistic predictions of the effects of the compounds. Therefore, we suggest the application in the industry of the protocols designed here. If the three IC_{50} values are similar, then the IC_{50} is a good indicator of the blocking effects of the compound and it can be used to predict its proarrhythmic risk, by using the Tx index[21] for example. Otherwise, study of the kinetics and state-dependent binding would be needed to better characterize it, and the formulation of mathematical models describing drug channel interactions would be worthy.

4.4 *Limitations*

Our work suggests the use of three voltage protocols instead of one when assessing the blocking potential of drugs. We have applied them to a wide range of virtual drugs and to two off-the-shelf drugs. Although it is not possible to experimentally reproduce our simulations, our work would also benefit from experiments with more types of drugs.

We have accounted for the effect of the temperature on the transition rates between the channel states. However, the influence of temperature on binding and unbinding rates of the virtual drugs have not been included as there is not a universal dependence followed by all compounds.

It is to mention that there are factors affecting data interpretation in ligand binding assays under equilibrium conditions that must be considered when designing and performing experiments to obtain Hill plot curves, such as ligand depletion, non-attainment of equilibrium, buffer composition and the temperature at which the assay is conducted[35].

All in all, we believe that our three-protocol hERG-IC_{50} assay would improve the evaluation of the proarrhythmic risk of drugs in the early stages of drug development.

5. Conclusions

Our work reveals that evaluation of the blocking potency of drugs in the early stages of drug development could be improved by the use of our three-protocol hERG-IC_{50} assay, which was designed to reveal the dissimilarities in the affinity of the drug to the different conformational states of the channel. Our results show that the influence of the stimulation protocol on IC_{50} evaluation depends on the specific I_{Kr}-drug interaction. In some cases, the three IC_{50} values registered for a compound are the same or very similar, then, the IC_{50} could be used as an estimator of the inhibitory potency. However, in other cases, the IC_{50} estimated by two different protocols could vary as much as two orders of magnitude. Then, kinetics and state-dependent properties would be also necessary to predict drug effects. Importantly, as the protocol that provided the

maximum IC_{50} was specific to the drug, the design of a "standard" protocol that provides as representative IC_{50} value for any compound becomes pointless. To sum up, adoption of our hERG-IC_{50} assay on the methods of routinely evaluating the effects of a drug on hERG channels on safety pharmacology would ultimately result in more accurate clinical predictions.

Supporting Information. Supporting Information available:

- Figure S1: Maximum IC_{50} ratios for each simulated drug obtained with our protocols and with Yao, et al. 2005 protocols at 22ºC.

- Figure S2: Maximum IC_{50} ratios obtained with our proposed protocols at 35ºC and comparison with 22ºC.

- Figure S3: Simulated steady state pseudo-ECGs for moxifloxacin and dofetilide

- Figure S4: Simulated Hill plots for each type of the prototypical drugs binding to two states with state-dependent affinities using the proposed protocols at 22ºC using the Lee et al. hERG model[19].

- Figure S5: Simulated Hill plots for each type of the prototypical drugs binding to two states with state-dependent affinities using the proposed protocols at 22ºC using the Li et al. hERG model[29].

- Figure S6: Simulated Hill plots for unstuck and stuck Inactivated_s using the three ionic channel models: Fink et al[16], Lee et al. model[19] and Li et al.[29].

AUTHOR INFORMATION

Corresponding Author

Lucia Romero*.

Centro de Investigación e Innovación en Bioingeniería (Ci2B),

Universitat Politècnica de València,

Camino de Vera s/n, 46022, Valencia, SPAIN.

Tel: +34 96 3877000 ext. 76024.

e-mail: lromero@ci2b.upv.es

Author Contributions

The manuscript was written through contributions of all authors. All authors have given approval to the final version of the manuscript.

ACKNOWLEDGMENT

This work was partially supported by the Dirección General de Política Científica de la Generalitat Valenciana (PROMETEU2016/088), Ministerio de Economía y Competitividad and Fondo Europeo de Desarrollo Regional (FEDER) DPI2015-69125-R (MINECO/FEDER, UE) as well as Ayuda a Primeros Proyectos de Investigación (PAID-06-18), Vicerrectorado de Investigación. Innovación y Transferencia de la Universitat Politècnica de València (UPV), València, Spain. The research was also supported by the National Institutes of Health 1R01HL128537-01A1.

ABBREVIATIONS

C_{AVG}, the average of the probabilities of the three closed states; CiPA, Comprehensive in vitro Pro-arrhythmia Assay; ClosedO, drug binding simultaneously to both the open and closed states with higher affinity to the closed state; CO, drug binding simultaneously to both the open and closed states with the same affinity to both states; COI, drug binding simultaneously all states with the same affinity; ClosedOI, drug binding simultaneously with higher affinity to the closed state; hERG, human ether-à-go-go-related gene; I_{AVG}, the average of the probability of the inactivated state; InactivO, drug binding simultaneously to both the inactivated and open states with higher affinity to the inactivated state; InactivOC, drug binding simultaneously all states with higher affinity to the inactivated state; IO, drug binding simultaneously to both the inactivated and open states with the same affinity to both states; IC_{50}, drug concentration that obstructs the 50% of the channels; I_{Kr}, rapid component of the delayed rectifier current; O_{AVG}, the average of the probability of the open state; OpenC, drug binding simultaneously to both the open and closed states with higher affinity to the open state; OpenCI, drug binding simultaneously all states with higher affinity to the inactivated state; OpenI, drug binding simultaneously to both the open and inactivated states with higher affinity to the open state; Stuck drug, drug that does not allow bound channels to change their conformational state unless unbinding occurs; TdP, torsade de pointes; Unstuck drug, drug that allows bound channels to change their conformational.

REFERENCES

(1) Gintant, G. A. Preclinical Torsades-de-Pointes Screens: Advantages and Limitations of Surrogate and Direct Approaches in Evaluating Proarrhythmic Risk. *Pharmacol. Ther.* **2008**, *119*, 199–209. https://doi.org/10.1016/j.pharmthera.2008.04.010.

(2) Food and Drug Administration. International Conference on Harmonisation; Guidance on

S7B Nonclinical Evaluation of the Potential for Delayed Ventricular Repolarization (QT Interval Prolongation) by Human Pharmaceuticals. *Fed. Regist.* **2005**, *70*, 61133–61134.

(3) Witchel, H. J.; Milnes, J. T.; Mitcheson, J. S.; Hancox, J. C. Troubleshooting Problems with in Vitro Screening of Drugs for QT Interval Prolongation Using HERG K+ Channels Expressed in Mammalian Cell Lines and Xenopus Oocytes. *J. Pharmacol. Toxicol. Methods* **2002**, *48*, 65–80. https://doi.org/10.1016/S1056-8719(03)00041-8.

(4) Kirsch, G. E.; Trepakova, E. S.; Brimecombe, J. C.; Sidach, S. S.; Erickson, H. D.; Kochan, M. C.; Shyjka, L. M.; Lacerda, A. E.; Brown, A. M. Variability in the Measurement of HERG Potassium Channel Inhibition: Effects of Temperature and Stimulus Pattern. *J. Pharmacol. Toxicol. Methods* **2004**, *50*, 93–101. https://doi.org/10.1016/j.vascn.2004.06.003.

(5) Yao, J.-A.; Du, X.; Lu, D.; Baker, R. L.; Daharsh, E.; Atterson, P. Estimation of Potency of HERG Channel Blockers: Impact of Voltage Protocol and Temperature. *J. Pharmacol. Toxicol. Methods* **2005**, *52*, 146–153. https://doi.org/10.1016/j.vascn.2005.04.008.

(6) Stork, D.; Timin, E. N.; Berjukow, S.; Huber, C.; Hohaus, A.; Auer, M.; Hering, S. State Dependent Dissociation of HERG Channel Inhibitors. *Br. J. Pharmacol.* **2007**, *151*, 1368–1376. https://doi.org/10.1038/sj.bjp.0707356.

(7) Hancox, J. C.; McPate, M. J.; El Harchi, A.; Zhang, Y. H. The HERG Potassium Channel and HERG Screening for Drug-Induced Torsades de Pointes. *Pharmacol. Ther.* **2008**, *119*, 118–132. https://doi.org/10.1016/j.pharmthera.2008.05.009.

(8) Dumaine, R.; Roy, M. L.; Brown, A. M. Blockade of HERG and Kv1.5 by Ketoconazole. *J. Pharmacol. Exp. Ther.* **1998**, *286*, 727–735.

(9) Milnes, J. T.; Dempsey, C. E.; Ridley, J. M.; Crociani, O.; Arcangeli, A.; Hancox, J. C.;

Witchel, H. J. Preferential Closed Channel Blockade of HERG Potassium Currents by Chemically Synthesised BeKm-1 Scorpion Toxin. *FEBS Lett.* **2003**, *547*, 20–26.

(10) Kim S, Thiessen PA, Bolton EE2, Chen J, Fu G, Gindulyte A, Han L, He J, He S, Shoemaker BA, Wang J, Yu B, Zhang J, Bryant SH; PubChem Substance and Compound Databases. *Nucleic Acids Res.* **2016**, *44*, D1202-1213. https://doi.org/10.1093/nar/gkv951.

(11) Wishart DS, Feunang YD, Guo AC, Lo EJ, Marcu A, Grant JR, Sajed T, Johnson D, Li C, Sayeeda Z, Assempour N, Iynkkaran I, Liu Y, Maciejewski A, Gale N, Wilson A, Chin L, Cummings R, Le D, Pon A, Knox C, Wilson M; DrugBank 5.0: A Major Update to the DrugBank Database for 2018. *Nucleic Acids Res.* **2018**, *46*, D1074–D1082. https://doi.org/10.1093/nar/gkx1037.

(12) Milnes, J. T.; Witchel, H. J.; Leaney, J. L.; Leishman, D. J.; Hancox, J. C. Investigating Dynamic Protocol-Dependence of HERG Potassium Channel Inhibition at 37ºC: Cisapride Versus Dofetilide. *J. Pharmacol. Toxicol. Methods* **2010**, *61*, 178–191. https://doi.org/10.1016/j.vascn.2010.02.007.

(13) Lee, W.; Windley, M. J.; Perry, M. D.; Vandenberg, J. I.; Hill, A. P. Protocol-Dependent Differences in IC50 Values Measured in Human Ether-Á-Go-Go-Related Gene Assays Occur in a Predictable Way and Can Be Used to Quantify State Preference of Drug Binding. *Mol. Pharmacol.* **2019**, *95*, 537–550. https://doi.org/10.1124/mol.118.115220.

(14) Carmeliet, E. Voltage- and Time-Dependent Block of the Delayed K+ Current in Cardiac Myocytes by Dofetilide. *J. Pharmacol. Exp. Ther.* **1992**, *262*, 809–817.

(15) Mitcheson, J. S.; Chen, J.; Sanguinetti, M. C. Trapping of a Methanesulfonanilide by Closure of the HERG Potassium Channel Activation Gate. *J. Gen. Physiol.* **2000**, *115*, 229–240. https://doi.org/10.1085/jgp.115.3.229.

(16) Fink, M.; Noble, D.; Virag, L.; Varro, A.; Giles, W. R. Contributions of HERG K+ Current to Repolarization of the Human Ventricular Action Potential. *Prog. Biophys. Mol. Biol.* **2008**, *96*, 357–376. https://doi.org/10.1016/j.pbiomolbio.2007.07.011.

(17) Romero, L.; Trenor, B.; Yang, P.-C.; Saiz, J.; Clancy, C. E. In Silico Screening of the Impact of HERG Channel Kinetic Abnormalities on Channel Block and Susceptibility to Acquired Long QT Syndrome. *J. Mol. Cell. Cardiol.* **2015**, *87*, 271–282.

(18) Colquhoun, D.; Dowsland, K. a; Beato, M.; Plested, A. J. R. How to Impose Microscopic Reversibility in Complex Reaction Mechanisms. *Biophys. J.* **2004**, *86*, 3510–3518. https://doi.org/10.1529/biophysj.103.038679.

(19) Lee, W.; Mann, S. A.; Windley, M. J.; Imtiaz, M. S.; Vandenberg, J. I.; Hill, A. P. In-Silico Assessment of Kinetics and State Dependent Binding Properties of Drugs Causing Acquired LQTS. *Prog. Biophys. Mol. Biol.* **2016**, *120*, 89–99. https://doi.org/10.1016/j.pbiomolbio.2015.12.005.

(20) Ellinwood, N.; Dobrev, D.; Morotti, S.; Grandi, E. Revealing Kinetics and State-Dependent Binding Properties of IKur-Targeting Drugs That Maximize Atrial Fibrillation Selectivity. *Chaos* **2017**, *27*, 093918. https://doi.org/10.1063/1.5000226.

(21) Romero, L.; Cano, J.; Gomis-Tena, J.; Trenor, B.; Sanz, F.; Pastor, M.; Saiz, J. In Silico QT and APD Prolongation Assay for Early Screening of Drug-Induced Proarrhythmic Risk. *J. Chem. Inf. Model.* **2018**, *58*, 867–878. https://doi.org/10.1021/acs.jcim.7b00440.

(22) O'Hara, T.; Virág, L.; Varró, A.; Rudy, Y. Simulation of the Undiseased Human Cardiac Ventricular Action Potential: Model Formulation and Experimental Validation. *PLoS Comput. Biol.* **2011**, *7*, e1002061. https://doi.org/10.1371/journal.pcbi.1002061.

(23) Mirams, G. R.; Cui, Y.; Sher, A.; Fink, M.; Cooper, J.; Heath, B. M.; McMahon, N. C.;

Gavaghan, D. J.; Noble, D. Simulation of Multiple Ion Channel Block Provides Improved Early Prediction of Compounds' Clinical Torsadogenic Risk. *Cardiovasc. Res.* **2011**, *91*, 53–61. https://doi.org/10.1093/cvr/cvr044.

(24) Obiol-Pardo, C.; Gomis-Tena, J.; Sanz, F.; Saiz, J.; Pastor, M. A Multiscale Simulation System for the Prediction of Drug-Induced Cardiotoxicity. *J. Chem. Inf. Model.* **2011**, *51*, 483–492. https://doi.org/10.1021/ci100423z.

(25) Mirams, G. R.; Davies, M. R.; Brough, S. J.; Bridgland-Taylor, M. H.; Cui, Y.; Gavaghan, D. J.; Abi-Gerges, N. Prediction of Thorough QT Study Results Using Action Potential Simulations Based on Ion Channel Screens. *J. Pharmacol. Toxicol. Methods* **2014**, *70*, 246–254. https://doi.org/10.1016/j.vascn.2014.07.002.

(26) Lancaster, M. C.; Sobie, E. A. Improved Prediction of Drug-Induced Torsades de Pointes Through Simulations of Dynamics and Machine Learning Algorithms. *Clin. Pharmacol. Ther.* **2016**, *100*, 371–379. https://doi.org/10.1002/cpt.367.

(27) Elkins, R. C.; Davies, M. R.; Brough, S. J.; Gavaghan, D. J.; Cui, Y.; Abi-Gerges, N.; Mirams, G. R. Variability in High-Throughput Ion-Channel Screening Data and Consequences for Cardiac Safety Assessment. *J. Pharmacol. Toxicol. Methods* **2013**, *68*, 112–122. https://doi.org/10.1016/j.vascn.2013.04.007.

(28) Alexandrou, A. J.; Duncan, R. S.; Sullivan, A.; Hancox, J. C.; Leishman, D. J.; Witchel, H. J.; Leaney, J. L. Mechanism of HERG K+ Channel Blockade by the Fluoroquinolone Antibiotic Moxifloxacin. *Br. J. Pharmacol.* **2006**, *147*, 905–916. https://doi.org/10.1038/sj.bjp.0706678.

(29) Li, Z.; Dutta, S.; Sheng, J.; Tran, P. N.; Wu, W.; Colatsky, T. A Temperature-Dependent in Silico Model of the Human Ether-à-Go-Go-Related (HERG) Gene Channel. *J. Pharmacol.*

Toxicol. Methods 81, 233–239. https://doi.org/10.1016/j.vascn.2016.05.005.

(30) Sager, P. T.; Gintant, G.; Turner, J. R.; Pettit, S.; Stockbridge, N. Rechanneling the Cardiac Proarrhythmia Safety Paradigm: A Meeting Report from the Cardiac Safety Research Consortium. *Am. Heart J.* **2014**, *167*, 292–300. https://doi.org/10.1016/j.ahj.2013.11.004.

(31) Windley, M. J.; Mann, S. A.; Vandenberg, J. I.; Hill, A. P. Temperature Effects on Kinetics of Kv11.1 Drug Block Have Important Consequences for in Silico Proarrhythmic Risk Prediction. *Mol. Pharmacol.* **2016**, *90*, 1–11. https://doi.org/10.1124/mol.115.103127.

(32) Li, Z.; Dutta, S.; Sheng, J.; Tran, P. N.; Wu, W.; Chang, K.; Mdluli, T.; Strauss, D. G.; Colatsky, T. Improving the In Silico Assessment of Proarrhythmia Risk by Combining HERG (Human Ether-à-Go-Go-Related Gene) Channel-Drug Binding Kinetics and Multichannel Pharmacology. *Circ. Arrhythm. Electrophysiol.* **2017**, *10*, e004628. https://doi.org/10.1161/CIRCEP.116.004628.

(33) Dutta, S.; Chang, K. C.; Beattie, K. A.; Sheng, J.; Tran, P. N.; Wu, W. W.; Wu, M.; Strauss, D. G.; Colatsky, T.; Li, Z. Optimization of an In Silico Cardiac Cell Model for Proarrhythmia Risk Assessment. *Front. Physiol.* **2017**, *8*, 616. https://doi.org/10.3389/fphys.2017.00616.

(34) Windley, M. J.; Abi-Gerges, N.; Fermini, B.; Hancox, J. C.; Vandenberg, J. I.; Hill, A. P. Measuring Kinetics and Potency of HERG Block for CiPA. *J. Pharmacol. Toxicol. Methods* **2017**, *87*, 99–107. https://doi.org/10.1016/j.vascn.2017.02.017.

(35) Hulme, E. C.; Trevethick, M. A. Ligand Binding Assays at Equilibrium: Validation and Interpretation. *Br. J. Pharmacol.* **2010**, *161*, 1219–1237. https://doi.org/10.1111/j.1476-5381.2009.00604.x.

Table of Contents

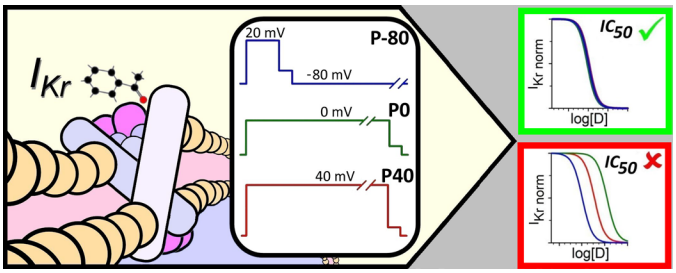

Supporting Information

When Does the IC_{50} Accurately Assess the Blocking Potency of a Drug?

Julio Gomis-Tena, Brandon M. Brown, Jordi Cano, Beatriz Trenor, Pei-Chi Yang, Javier Saiz, Colleen E. Clancy, Lucia Romero[*].

[a]Centro de Investigación e Innovación en Bioingeniería (Ci2B), Universitat Politècnica de València, Camino de Vera, s/n, 46022, Valencia, Spain.

[b]Department of Pharmacology, One Shields Avenue, University of California, Davis, Davis, CA 95616-8636

*Corresponding Author e-mail: lurope@ci2b.upv.es

Table S1. Kinetic rates of the simulated drug-I_{Kr} interactions. Corresponding Markovian models (first column) are shown in *Figure 1 of the main article,* and k and r are the diffusion and the dissociation rates, respectively.

Configuration	Name	Closed		Open		Inactivated	
		k$(\mu M^{-1}s^{-1})$	**r**(s^{-1})	**k**$(\mu M^{-1}s^{-1})$	**r**(s^{-1})	**k**$(\mu M^{-1}s^{-1})$	**r**(s^{-1})
A and B	Closed_s	1	0.01				
	Closed_m	1	0.1				
	Closed_f	1	1				
	Closed_ff	10	10				
C and D	Open_s			1	0.01		
	Open_m			1	0.1		
	Open_f			1	1		
	Open_ff			10	10		
E and F	Inactivated_s					1	0.01
	Inactivated_m					1	0.1
	Inactivated_f					1	1
	Inactivated_ff					10	10
G and H	ClosedO_sss	1	0.001	1	0.1		
	ClosedO_ss	1	0.003	1	0.3		
	ClosedO_s	1	0.01	1	1		
	ClosedO_m	1	0.1	1	10		
	ClosedO_f	1	1	1	100		
	ClosedO_ff	10	10	10	1000		
	OpenC_sss	1	0.1	1	0.001		
	OpenC_ss	1	0.3	1	0.003		
	OpenC_s	1	1	1	0.01		
	OpenC_m	1	10	1	0.1		
	OpenC_f	1	100	1	1		
	OpenC_ff	10	1000	10	10		
	CO_sss	1	0.001	1	0.001		
	CO_ss	1	0.003	1	0.003		

	CO_s	1	0.01	1	0.01		
	CO_m	1	0.1	1	0.1		
	CO_f	1	1	1	1		
	CO_ff	10	10	10	10		
I and J	OpenI_sss			1	0.001	1	0.1
	OpenI_ss			1	0.003	1	0.3
	OpenI_s			1	0.01	1	1
	OpenI_m			1	0.1	1	10
	OpenI_f			1	1	1	100
	OpenI_ff			10	10	10	1000
	InactivO_sss			1	0.1	1	0.001
	InactivO_ss			1	0.3	1	0.003
	InactivO_s			1	1	1	0.01
	InactivO_m			1	10	1	0.1
	InactivO_f			1	100	1	1
	InactivO_ff			10	1000	10	10

Table S2. Kinetic rates of the simulated drug-I_{Kr} interactions. Corresponding Markovian models (first column) are shown in *Figure 1 of the main article,* and k and r are the diffusion and the dissociation rates, respectively.

Configuration	Name	Closed		Open		Inactivated	
		k$(\mu M^{-1}s^{-1})$	**r**(s^{-1})	**k**$(\mu M^{-1}s^{-1})$	**r**(s^{-1})	**k**$(\mu M^{-1}s^{-1})$	**r**(s^{-1})
I and J	IO_sss			1	0.001	1	0.001
	IO_ss			1	0.003	1	0.003
	IO_s			1	0.01	1	0.01
	IO_m			1	0.1	1	0.1
	IO_f			1	1	1	1
	IO_ff			10	10	10	10
K and L	ClosedOI_sss	1	0.001	1	0.1	1	0.1
	ClosedOI_ss	1	0.003	1	0.3	1	0.3
	ClosedOI_s	1	0.01	1	1	1	1
	ClosedOI_m	1	0.1	1	10	1	10
	ClosedOI_f	1	1	1	100	1	100
	ClosedOI_ff	10	10	10	1000	10	1000
	OpenCI_sss	1	0.1	1	0.001	1	0.1
	OpenCI_ss	1	0.3	1	0.003	1	0.3
	OpenCI_s	1	1	1	0.01	1	1
	OpenCI_m	1	10	1	0.1	1	10
	OpenCI_f	1	100	1	1	1	100
	OpenCI_ff	10	1000	10	10	10	1000
	InactivOC_sss	1	0.1	1	0.1	1	0.001
	InactivOC_ss	1	0.3	1	0.3	1	0.003
	InactivOC_s	1	1	1	1	1	0.01
	InactivOC_m	1	10	1	10	1	0.1
	InactivOC_f	1	100	1	100	1	1
	InactivOC_ff	10	1000	10	1000	10	10
	COI_sss	1	0.001	1	0.001	1	0.001
	COI_ss	1	0.003	1	0.003	1	0.003

	COI_s	1	0.01	1	0.01	1	0.01
	COI_m	1	0.1	1	0.1	1	0.1
	COI_f	1	1	1	1	1	1
	COI_ff	10	10	10	10	10	10

Figure S1. Maximum IC_{50} ratios for unstuck (top panel) and stuck (bottom panel) drugs obtained with our protocols (non-filled bars) and with Yao, et al. 2005[1] protocols (filled bars) at 22ºC.

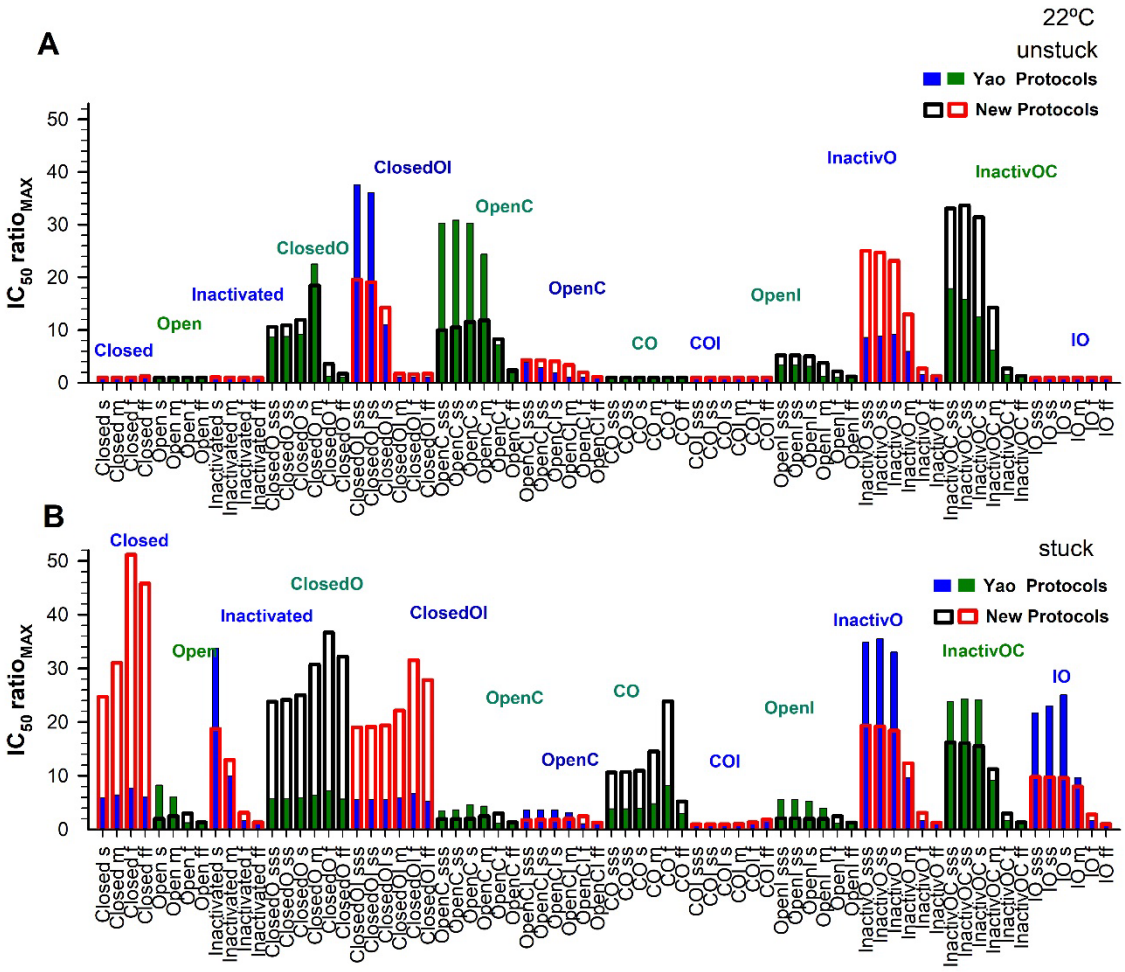

Figure S2. Maximum IC_{50} ratios obtained with our proposed protocols (P0, P40 and P-80) at 35ºC (A) and comparison with 22ºC (B). A: IC_{50} ratios for each prototypical drug at 35ºC. Filled (green and blue) and non-filled (black and red) bars for stuck and unstuck drugs, respectively. B: maximum IC_{50} ratios at 35ºC relative to those observed at 22ºC. In order to compare previous results directly to those obtained at 22ºC, the maximum IC_{50} ratio at 35ºC was normalized to the maximum IC_{50} ratio at 22ºC (ratio_35_22). Colored bars in Panel B are depicted from unity to the value of ratio_35_22. Stuck and unstuck refer to the state of the channel when the drug is bound.

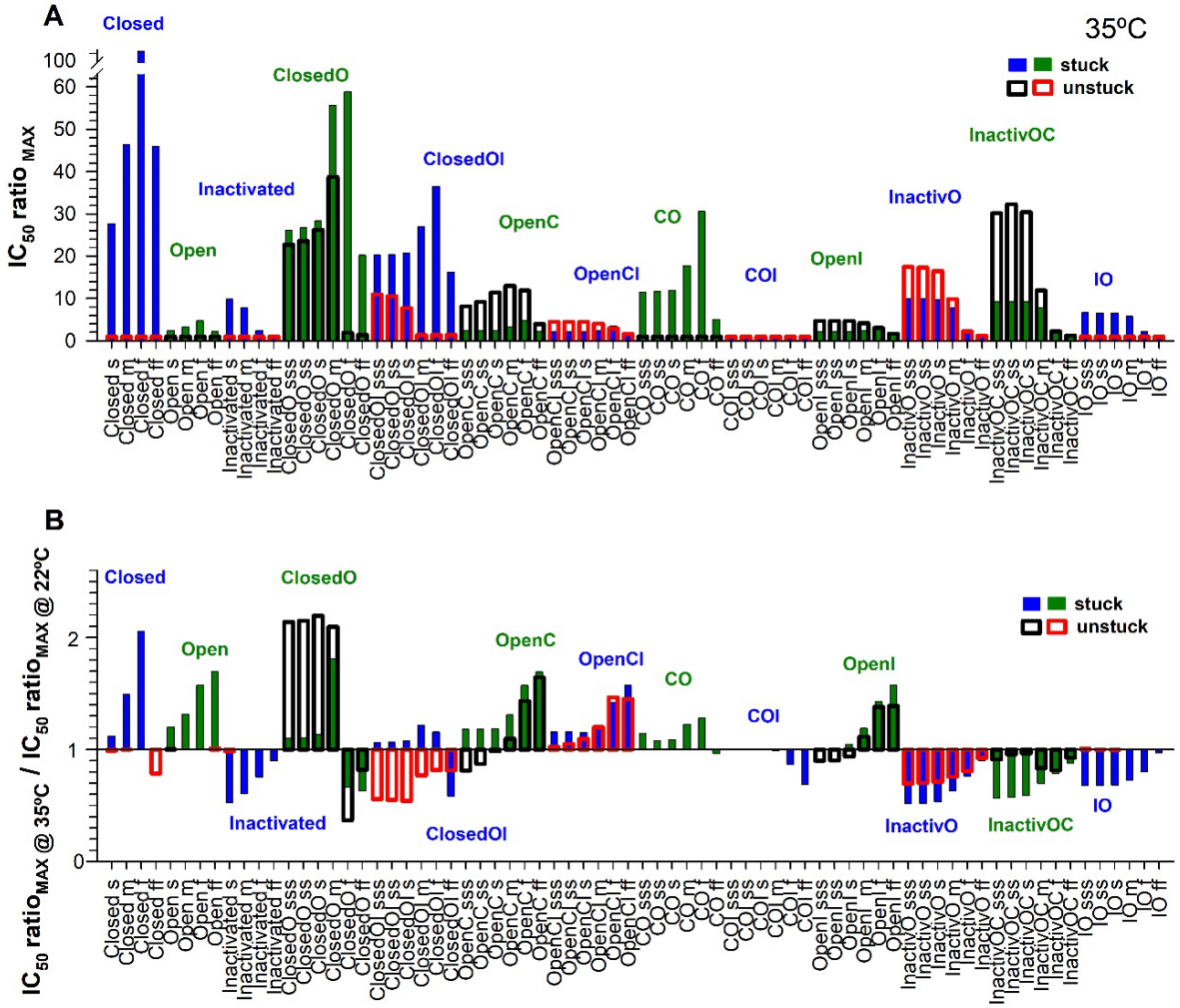

Figure S3. Simulated steady state pseudo-ECGs for moxifloxacin (top row) and dofetilide (bottom row). Simulated steady state pseudo-ECG in control (black) and in the presence of 6.228 μM of moxifloxacin and 2 nM of dofetilide considering the IC_{50} obtained using the P-80 (blue), P0 (red) and P40 (green).

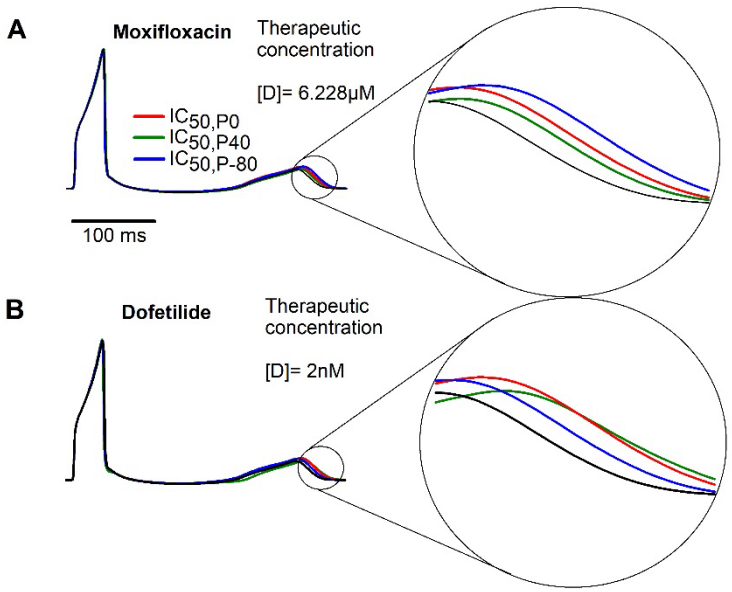

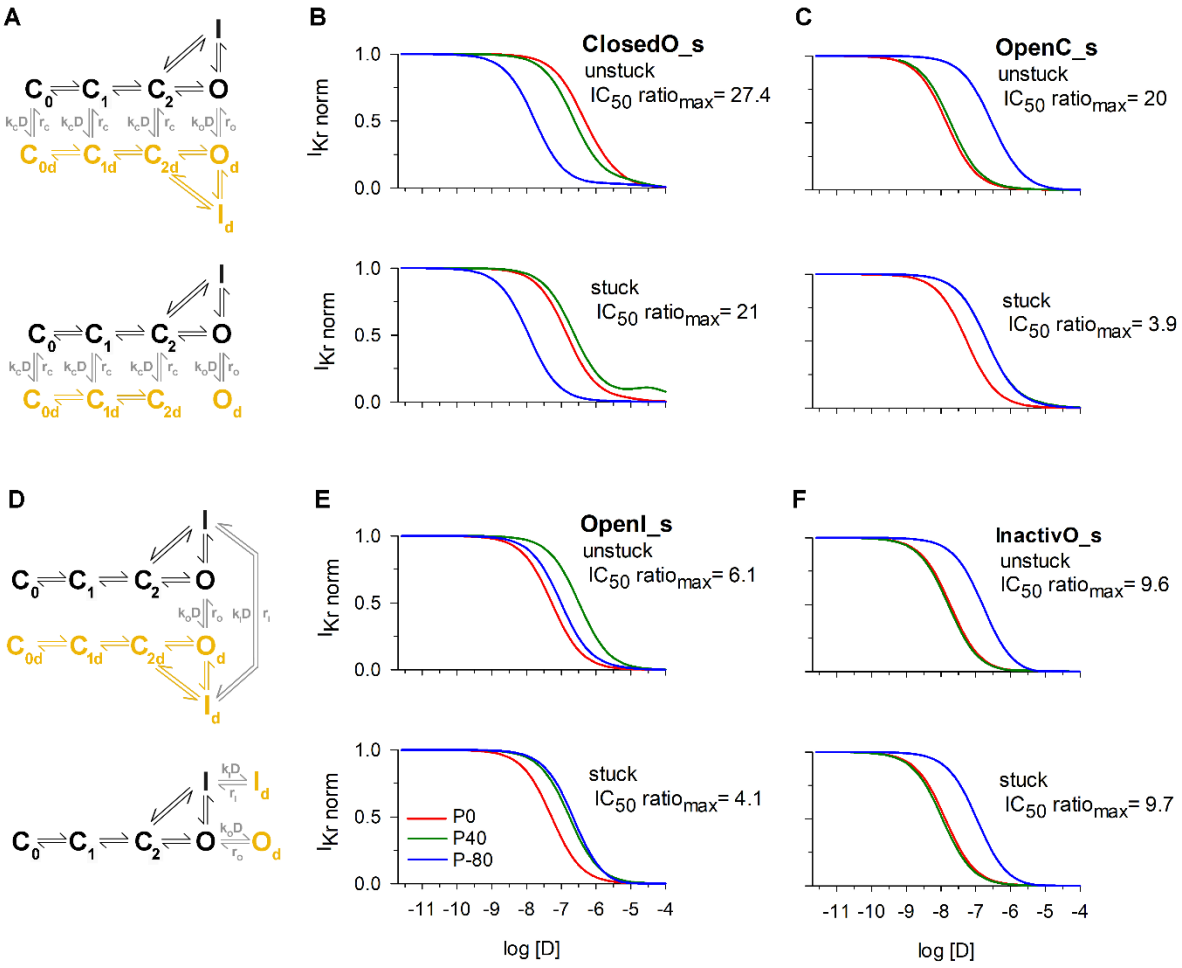

Figure S4. Simulated Hill plots for each type of the prototypical drugs binding to two states with state-dependent affinities using the proposed protocols: P-80 (blue), P0 (red) and P40 (green) at 22ºC using Lee et al. hERG model[2]. Left column shows the Markovian schemes of the drug-channel interactions of each row: unstuck (top) and stuck (bottom) variants of ClosedO_s (B), OpenC_s (C), OpenI_s (E) and InactivO_s (F). Unbound states are depicted in black and transitions between them are defined as in[2], drug bound states are depicted in yellow and transition between unbound and drug bound channels are depicted in gray. Microscopic reversibility was ensured by equaling the product of the rates going clockwise to the product going anticlockwise

in closed loops[3]. As drug-bound channels are electrically silent, which precludes the assessment of the transition rates between states, we modified the transition rates from I_d to O_d, from O_d to $C2_d$ and from I_d to $C2_d$ when appropriate. The maximum IC_{50} ratio for each drug is also indicated in each panel.

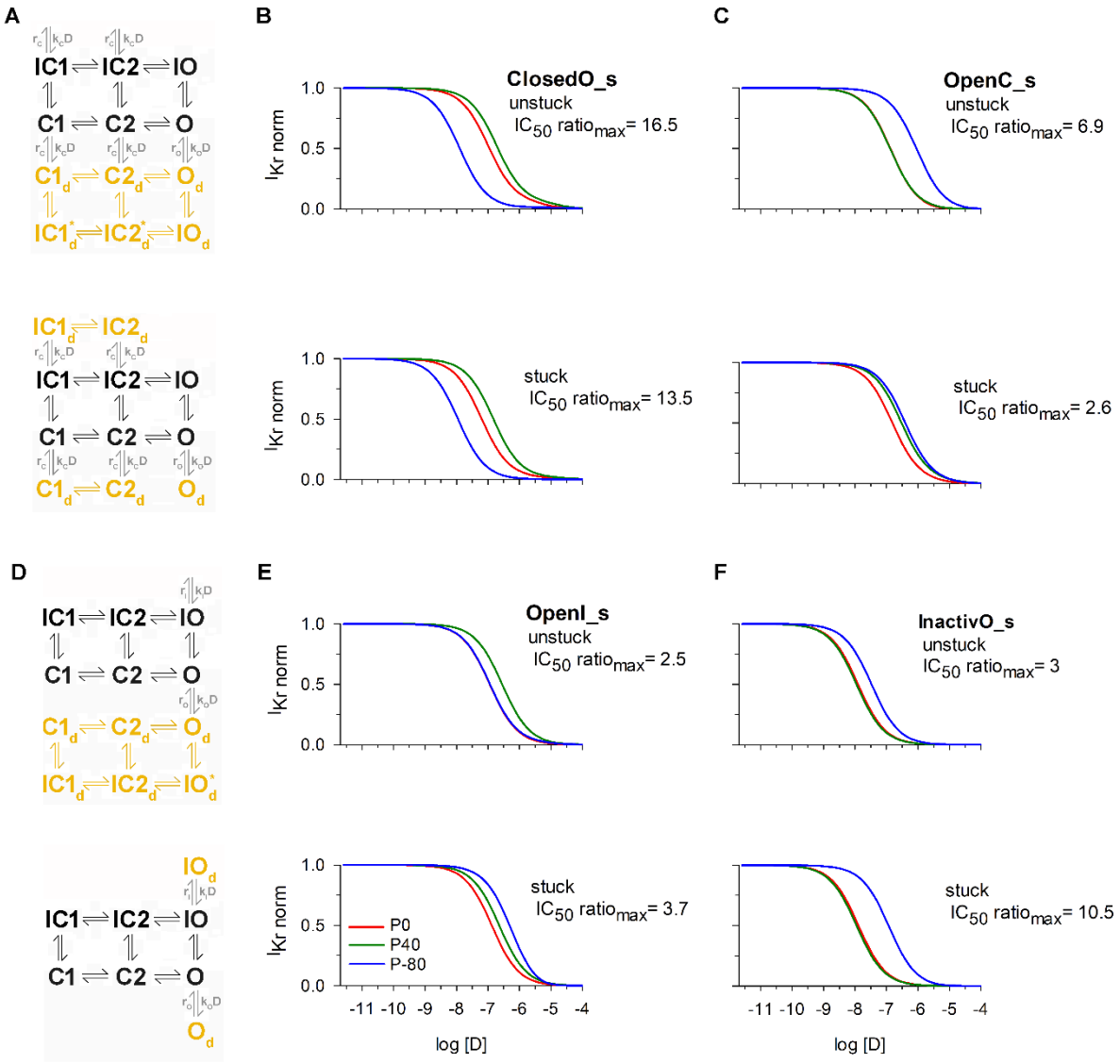

Figure S5. Simulated Hill plots for each type of the prototypical drugs binding to two states with state-dependent affinities using the proposed protocols: P-80 (blue), P0 (red) and P40 (green) at 22ºC using Li et al. hERG model[4]. Left column shows the Markovian schemes of the drug-channel interactions of each row: unstuck (top) and stuck (bottom) variants of ClosedO_s (B), OpenC_s (C), OpenI_s (E) and InactivO_s (F). Unbound states are depicted in black and transitions between them are defined as in[4], drug bound states are depicted in yellow and transition

between unbound and drug bound channels are depicted in gray. Transition rates between IC1 and $IC1_d$, IC2 and $IC2_d$ and IO and IO_d are depicted at the top of IC1, IC2 and IO and the asterisks in IC1d, IC2d and IO_d indicate that they are connected to IC1, IC2 and IO, respectively, by means of these transition rates (top panels in A and D). Microscopic reversibility was ensured by equaling the product of the rates going clockwise to the product going anticlockwise in closed loops[3]. As drug-bound channels are electrically silent, which precludes the assessment of the transition rates between states, we modified the transition rates from I_d to O_d, from O_d to $C2_d$ and from I_d to $C2_d$ when appropriate. The maximum IC_{50} ratio for each drug is also indicated in each panel.

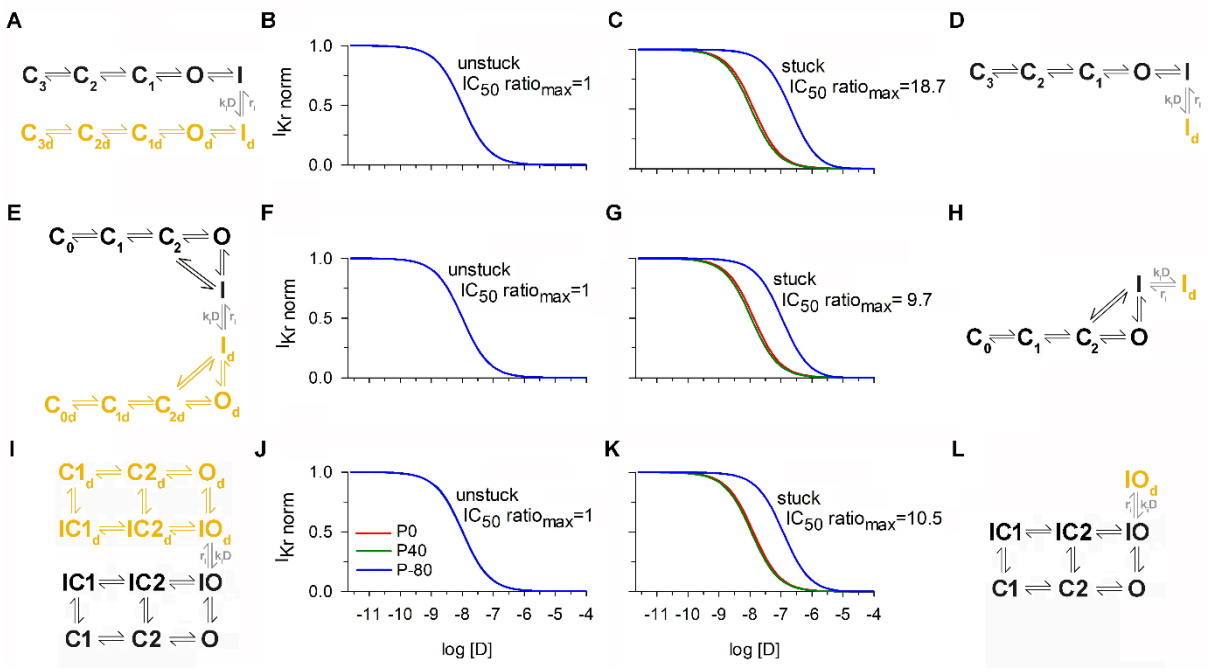

Figure S6. Simulated Hill plots for unstuck and stuck Inactivated_s using three ionic channel models: Fink et al[5] (B and C), Lee et al.[2] (F and G) and Li et al.[4] (J and K) models, and the corresponding Markovian schemes of the unstuck and stuck drug-channel interactions (A and D, E and H, and I and L, respectively). Unbound states are depicted in black, drug bound states are depicted in yellow and transition between unbound and drug bound channels are depicted in gray. The maximum IC_{50} ratio for each drug is also indicated in each panel.

References

(1) Yao, J.-A.; Du, X.; Lu, D.; Baker, R. L.; Daharsh, E.; Atterson, P. Estimation of Potency of HERG Channel Blockers: Impact of Voltage Protocol and Temperature. *J. Pharmacol. Toxicol. Methods* **2005**, *52*, 146–153. https://doi.org/10.1016/j.vascn.2005.04.008.

(2) Lee, W.; Mann, S. A.; Windley, M. J.; Imtiaz, M. S.; Vandenberg, J. I.; Hill, A. P. In-Silico Assessment of Kinetics and State Dependent Binding Properties of Drugs Causing Acquired LQTS. *Prog. Biophys. Mol. Biol.* **2016**, *120*, 89–99. https://doi.org/10.1016/j.pbiomolbio.2015.12.005.

(3) Colquhoun, D.; Dowsland, K. a; Beato, M.; Plested, A. J. R. How to Impose Microscopic Reversibility in Complex Reaction Mechanisms. *Biophys. J.* **2004**, *86*, 3510–3518. https://doi.org/10.1529/biophysj.103.038679.

(4) Li, Z.; Dutta, S.; Sheng, J.; Tran, P. N.; Wu, W.; Colatsky, T. A Temperature-Dependent in Silico Model of the Human Ether-à-Go-Go-Related (HERG) Gene Channel. *J. Pharmacol. Toxicol. Methods 81*, 233–239. https://doi.org/10.1016/j.vascn.2016.05.005.

(5) Fink, M.; Noble, D.; Virag, L.; Varro, A.; Giles, W. R. Contributions of HERG K+ Current to Repolarization of the Human Ventricular Action Potential. *Prog. Biophys. Mol. Biol.* **2008**, *96*, 357–376. https://doi.org/10.1016/j.pbiomolbio.2007.07.011.